To the Graduate Council:

I am submitting herewith a thesis written by Baskar Vairamohan entitled “State of Charge Estimation for Batteries”. I have examined the final electronic copy of this thesis for form and content and recommend that it can be accepted in partial fulfillment of the requirement for the degree of Master of Science, with a major in Electrical Engineering.

John Chiasson, Major Professor

We have read this thesis

and recommend its acceptance:

Leon.M.Tolbert

William.R.Hamel

Accepted for the council:

Anne Mayhew

Vice Provost and Dean of Graduate Studies

(Original signatures are on file with official student records.)

STATE OF CHARGE ESTIMATION FOR BATTERIES

A Thesis
Presented for the
Master of Science Degree
The University of Tennessee, Knoxville

Baskar Vairamohan
December 2002

Copyright © 2002 by Baskar Vairamohan
All rights reserved

Abstract

In this thesis, a methodology to accurately estimate the state of charge (SOC) of the batteries used in *Hybrid Electric Vehicles (HEV)* is proposed. A linear relationship exists between open circuit voltage (V_{OC}) and SOC. In the proposed scheme, a system theory approach is employed to identify the open circuit voltage of the battery, from which the state of charge of the battery is determined. This method is very unique because it estimates the V_{OC} of the battery in the vehicle even under load conditions. A state variable approach yields a set of non-linear time varying equations that describe the dynamics of the battery. This non-linear time varying system is reduced to a linear time varying system by making certain reasonable assumptions. The observability Gramian is calculated for the new linearized system from which V_{OC} is identified. The terminal voltage and the discharging current measurements are obtained from the battery with the help of ABC-150, a programmable power processing system. The SOC estimation of the battery under discharging conditions alone is considered in this thesis. The V_{OC} is then used to estimate the state of charge of the battery by exploiting the linear relationship between them. The results of applying the proposed technique are found to be comparable to the actual experimental results.

Dedication

I would like to dedicate my thesis work to my loving parents, Vairamohan and Jayakumari Vairamohan, whose love, moral support, motivation and encouragement helped me overcome all the difficulties that I encountered during the course of this work and achieve my goals.

Acknowledgements

I would like to take this opportunity to express my deep gratitude to my advisor and mentor Dr. John Chiasson for his constant help, support and guidance which has steered me towards my destination. His enthusiasm and new ideas have motivated me to explore new areas in the field of battery modeling.

I would like to thank Dr. Leon Tolbert and Dr. William Hamel for serving on my committee and providing me with valuable suggestions. I would like to express my sincere thanks to Dr. David Irick of Mechanical Engineering department, who helped me gather data from the laboratory.

My sincere thanks to Dr. Jay Farrell and Shuo Pang of the Electrical engineering department at the University of California Riverside, for their help and ideas which helped me overcome the difficulties in my thesis.

I thank Alexander Pal for providing me his SIMULINK model of Hybrid electric vehicle during the initial stages of my thesis, which gave me new ideas. Special thanks to my friends, Venkatesh Srinivasan, for proof reading my thesis, Sowmyan Rajagopalan and Kannan Kase for giving me valuable suggestions. My hearty thanks to all my friends and family members who encouraged me and supported me throughout the graduate course.

Last but not the least, all glory belongs to God. In Him, we all live, move and have our existence (Acts 17:28). He is worthy of all praise.

Table of Contents

1 INTRODUCTION 1

1.1 HEV Configurations 2

1.1.1 Series HEV Configuration 2

1.1.2 Parallel HEV Configuration 4

1.1.3 Dual Mode HEV Configuration 6

1.2 Thesis Objective 8

1.3 Thesis organization 10

2 MATHEMATICAL MODELING OF A BATTERY 12

2.1 Battery parameters 15

2.2 Various models available for battery modeling 17

2.2.1 Simple battery model 17

2.2.2 Resistive Thevenin battery model 19

2.2.3 Modified Thevenin equivalent battery model 20

2.3 Mathematical equations of the modified Thevenin's equivalent model 22

2.4 V_{OC} estimation strategy 30

2.5 SOC estimation strategy 32

2.6 Summary 32

3 SIMULATION OF THE BATTERY MODEL USING MATLAB 33

3.1 Simulation methods 33
3.1.1 Minimization Techniques 33
3.1.2 System Theory Approach - Observability Gramian Method 37
3.2 Simulation procedure 44
3.3 Simulation setup in SIMULINK 44
3.4 Function of OPTIMIZATION TOOLBOX 48
3.5 Summary 49
4 STATE OF CHARGE ESTIMATION WITH REAL-TIME BATTERY DATA 50
4.1 ABC-150-Battery emulator and test equipment 50
4.1.1 ROS Operating system 52
4.1.2 Various modes of operation 54
4.2 Experimental results 54
5 CONCLUSIONS AND SUMMARY 60
5.1 Summary of the thesis 60
5.2 Conclusion 61
5.3 Future work 62
LIST OF REFERENCES 64
APPENDICES 66
VITA 77

List of Figures

Figure 1 Series HEV configuration 3

Figure 2 Parallel HEV configuration 5

Figure 3 Dual mode HEV configuration 7

Figure 4 Battery and its components [Source: www.hepi.com] 13

Figure 5 Cross-sectional view of a typical sealed lead-acid battery [Source: www.hepi.com] 14

Figure 6 Simple battery model 18

Figure 7 Thevenin battery model 19

Figure 8 Modified Thevenin equivalent battery model 20

Figure 9 Battery discharging current Ib(t) used in simulation 31

Figure 10 Real battery terminal voltage Vb(t) 36

Figure 11 Simulink model of the battery 41

Figure 12 Interaction between various components in MATLAB 45

Figure 13 Sample SIMULINK block 47

Figure 14 Snapshot of ROS graphical test control 53

Figure 15 Result - 1: Battery terminal voltage $V_b(t)$, battery current $I_b(t)$ and

the estimated open circuit voltage $V_{OC}(t)$ using observability Gramian method 56

Figure 16 Result - 2: Battery terminal voltage $V_b(t)$, battery current $I_b(t)$ and the estimated open circuit voltage $V_{OC}(t)$ using observability Gramian method 57

Figure 17 Result - 1: Comparison of V_{OC} and SOC using Observability Gramian method 58

Figure 18 Result - 2: Comparison of V_{OC} and SOC estimated using Observability Gramian method 59

Chapter 1
Introduction

The automobile industry continues to grow by leaps and bounds, and due to the increase in the number of vehicles worldwide, air-pollution continues to increase. Though the automobile manufacturers have reduced the emission of greenhouse gases such as hydro-carbons, carbon monoxide, carbon dioxide etc., from the vehicles, they cannot produce a zero-emission vehicle unless they produce an electric vehicle (EV). An electric vehicle is an emission free, environment friendly vehicle. However, the electric vehicles remain unpopular among the consumers due to their lack of performance and their inability to travel long distances without being recharged. So, vehicles that embrace both the performance characteristics of the conventional automobile and the zero-emission characteristics of the electric vehicles are greatly being anticipated by the general consumers and the environmentalists alike. This lead manufacturers to come up with a vehicle that is acceptable by the consumers and also meets the performance of the conventional vehicle with much less emissions. Such vehicles are branded as *Hybrid Electric Vehicles (HEV)*, the name being derived from their ability to run in either gasoline mode or electric mode or both. The electric motor in the hybrid electric vehicle assists the gasoline engine during acceleration and receives its power from a dedicated battery pack. The beauty of the HEV is that energy can be fed back into the battery for storage, e.g., during regenerative braking (which is otherwise wasted as heat in a conventional vehicle). Leading car manu-

facturers like Toyota and Honda have already started mass producing HEV cars, Prius and Insight respectively, which are now becoming very popular among the consumers for their incredible mileage and less emissions. In the coming years many more automobile manufacturers will come up with their own HEVs. Currently, the sport-utility vehicles (SUVs) are the largest gas consuming vehicles and one of the most popular vehicles in USA. It will be a great breakthrough if hybrid SUVs come into the market, and it will certainly become a reality in the near future.

1.1 HEV Configurations

In this section, a brief description about various HEV configurations available in the market is presented. The three main configurations are the series, parallel and the dual-mode configurations and the explanation of each one of them with their merits and demerits follows.

1.1.1 Series HEV Configuration

In *series HEV* configuration, only the electric motor is connected to the drive train and thus the vehicle is entirely driven by the electric motor. The Internal Combustion (IC) engine drives an electric generator (commonly known as alternator), which then supplies the electric power to the motor and battery pack. The IC engine will turn off if the battery is fully charged. In some cases, the electric power supply for the electric motor can come from both battery and the engine-generator set. As only the electric motor is connected

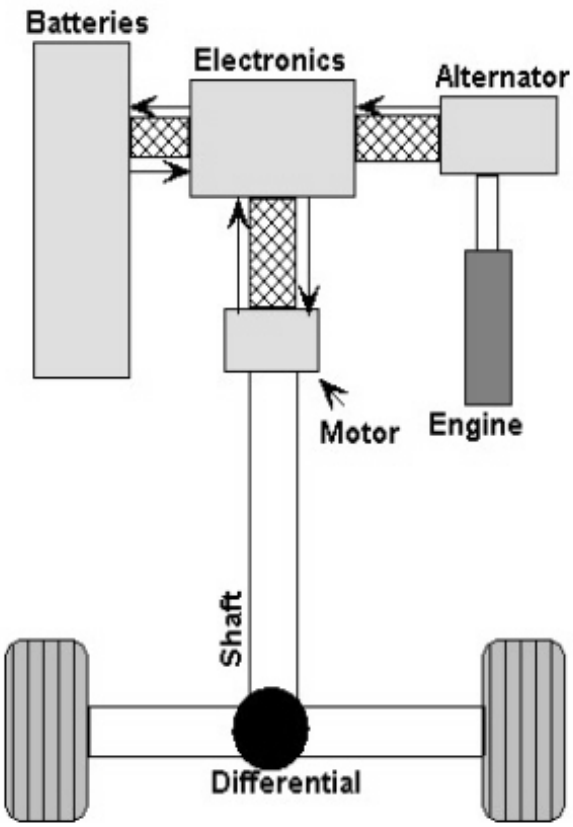


Figure 1. Series HEV configuration

to the drive train, the IC engine can run at an optimum speed to run the generator thus greatly reducing the emissions. The batteries can either be charged off-board, by external DC power link from the electric-grid, or on-board, with the help of an alternator and an IC engine. In this setup, it is possible to design the operation such that the IC engine never idles and thus the overall emissions are reduced. The schematics of series HEV is shown in Figure 1.

The *hatched links* that connect the alternator (generator), battery pack, electric motor

and the electronic interface represents the electric flow in the system whereas the *non-hatched links* represents the mechanical energy flow in the system. The directions shown by the arrows represent the direction of the flow of electric energy. This convention is followed throughout this chapter. It can be seen that the IC engine is connected to the alternator (generator) which in turn is connected to the battery pack and electric motor through a electronic control unit. This scheme allows the electric motor to get its power from either battery pack or the alternator or both as per the battery state of charge and vehicle acceleration requirements.

Advantages:

- Low emission drive is possible most of the time
- Engine can run more efficiently because it is not directly connected to the drive train

Disadvantages:

- The vehicle needs a full-sized electric motor, an electric generator and an IC engine, each of which can supply the required power for the vehicle.
- The vehicle is only driven by the electric motor, which places great constraints on the battery pack and in particular requires large battery capacities.

1.1.2 Parallel HEV Configuration

In the *parallel HEV* configuration there are two power paths for the drive train, while one comes from the engine the other comes from the electric motor. During short trips the

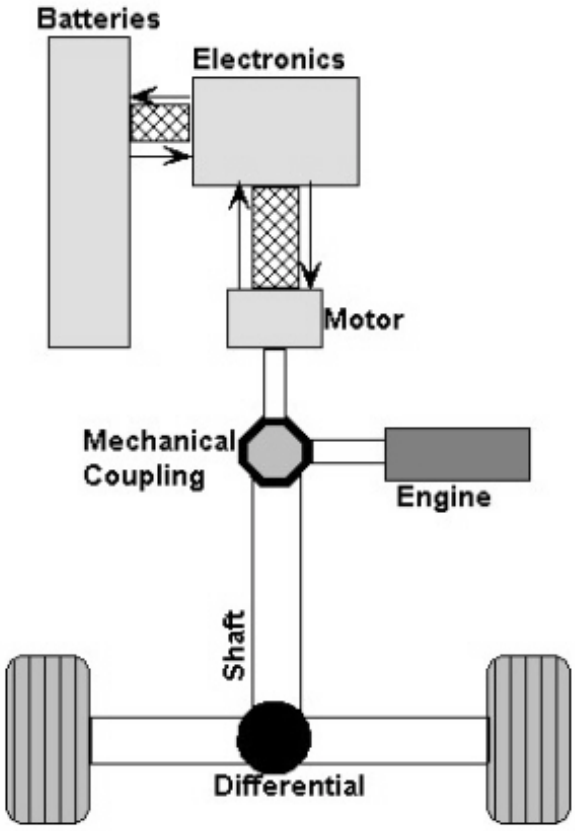


Figure 2. Parallel HEV configuration

electric motor can power the vehicle, while during long drives the IC engine can power the vehicle. The vehicle can thus have engine only, motor only or a combination of engine and motor mode of operation. The electric motor can also assist the engine during hill climbs and vehicle accelerations, thus the rating of the IC engine can be reduced. This configuration is illustrated in Figure 2.

In parallel HEV configurations, the drive train is connected to the electric motor and engine through a mechanical coupling or an angle gear. These vehicles do not require a

generator (as in the case of series HEV configuration) and they can be connected to an electric grid (off-board) for recharging the batteries. The electric motor can be made to act as generator via a mechanical clutch which can then be used for regenerative braking.

Advantages:

- In this configuration, the battery size can be small, as both the engine and motor are connected to the drive train.
- The performance is very much comparable to conventional vehicles due to dual power sources.
- The constraints on the battery pack and the electric motor are relaxed in this configuration.

Disadvantage:

- The vehicle cannot get full acceleration support from the electric motor when the battery pack charge is low. For example, when pulling a boat/ trailer up an inclination, the vehicle must rely on the IC engine as the battery pack will deplete quickly.

1.1.3 Dual Mode HEV Configuration

Dual mode hybrid vehicles are parallel hybrids, but differ from them in the aspect that an alternator (generator) is coupled to the IC engine that charges the battery. During normal operation, the IC engine turns both the drivetrain and the generator, which in turn feeds the battery pack through the electronic control unit. During full-throttle acceleration, the

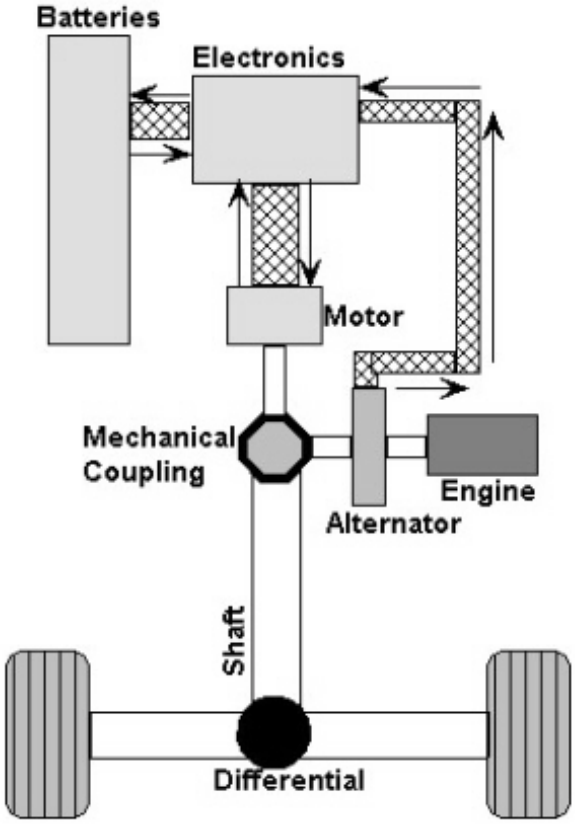


Figure 3. Dual mode HEV configuration

electric motor gets power from the battery and assists the IC engine to attain the requested acceleration. Choosing a full size electric motor, which uses the IC engine only for charging the battery and occasionally for turning the wheels, can reduce tail pipe emissions and this can be achieved with the help of a mechanical clutch (this method is essentially running the system as a series HEV). Thus, this configuration exhibits dual capability and hence the name dual mode HEV configuration. The schematic of the dual-mode HEV configuration is shown in Figure 3.

Advantage:

- It has both the advantages of the series and parallel configurations

Disadvantage:

- It needs more components such as an electric motor, an electric generator, an IC engine and a battery pack, for its operation which makes it more expensive.

1.2 Thesis Objective

A key component responsible for reducing the emissions in the three configurations mentioned in the earlier section, is the electric motor. In order to efficiently run the electric motor, the battery should be charged above valid limits, for example $20\% \leq SOC(\%) \leq 95\%$. So a need for measuring the charge (commonly known as state of charge) of the battery becomes very essential. Conventional gasoline vehicles have a fuel gauge to measure the fuel level, but as HEV runs on both gasoline and electricity, it needs a gauge to measure the available capacity of the battery. This will facilitate the vehicle control unit to be aware of the battery capacity accurately and help it maintain the state of charge within safe limits. Measuring the battery state of charge (SOC) is not an easy task because the SOC depends on many factors such as temperature, battery capacitance and battery internal resistance. In a HEV, charging and discharging of the battery is constantly taking place, therefore keeping track of the SOC is an essential but difficult task. The main objective of this thesis is to estimate the state of charge of the battery accurately and effectively. The

approach in this thesis is to basically estimate the open circuit voltage (V_{OC}) of the battery and then make use of a known (linear) relationship between state of charge and open circuit voltage to estimate the state of charge of the battery. The relationship between the V_{OC} and the SOC [1] is given by

$$v_{oc}(t) = aS(t) + b \tag{1.1}$$

$$S(t) = \frac{v_{oc}(t) - b}{a} \tag{1.2}$$

where $S(t)$ is the state of charge (%) of the battery, b is the battery terminal voltage when $S(t) = 0\%$, and a is obtained knowing the value of b and V_{OC} at $S(t) = 100\%$. Based on Equation (1.1), there is a great interest in using open circuit voltage to determine the SOC of the battery. But, in order to get the battery V_{OC}, the battery has to be disconnected from the load, which is not possible during the vehicle operation. To overcome this difficulty Farrell suggests a method [1], where the parameter V_{OC} can be estimated even under load conditions. He uses the Extended Kalman Filter (EKF) method [2] to identify V_{OC} and subsequently the state of charge of the battery. In the proposed method a new approach is employed where numerical analysis technique is used to obtain the V_{OC} and subsequently the SOC of the battery. A non-linear equation to estimate the battery terminal voltage is derived based on the dynamics of the modified Thevenin battery model obtained from [1]. The derived equation for the terminal voltage of the battery consists of a combination of battery parameters such as internal resistance (R_b), open circuit voltage (V_{OC}), charging/ discharging resistances (R_c/R_d), and the polarization capacitance (C). The battery terminal voltage and the current is measured with the help of ABC-150, a pro-

grammable power processing equipment. The OPTIMIZATION TOOLBOX from MATLAB, operates on the collected voltage and current data from the battery, to find an optimum value for the battery parameters in order to minimize the error between the measured terminal voltage and the estimated terminal voltage (as obtained from the non-linear terminal voltage equation) of the battery. The V_{OC}, which is identified by the OPTIMIZATION TOOLBOX, is then used to estimate the state of charge of the battery using the linear relationship between them. It should be noted that the SOC of the battery under discharging conditions alone is considered in this thesis.

1.3 Thesis organization

Chapter 2 discusses about the various models available for modeling the battery and why modified Thevenin model was chosen for the thesis. The mathematical equations behind the model were derived from the basic dynamics of the circuit model and the strategy adopted to estimate the V_{OC} and SOC are explained in this chapter.

Chapter 3 describes the methods that are chosen to estimate the V_{OC} of the battery, particularly the minimization techniques and system theory approach. Then the simulation setup in MATLAB and the toolbox are explained.

Chapter 4 elucidates the results obtained using the real-time battery data. It gives a brief description about ABC-150 and its role in the battery data measurements. It also explains the difficulties encountered while collecting the data and testing it with the numerical

method.

Finally, Chapter 5 presents the summary and conclusions of this work and opens up avenues for possible future work.

Chapter 2
Mathematical modeling of a battery

Batteries revolutionized the way electricity can be stored and paved the way for greater mobility in our day-to day lives. From portable cell phones to high-tech space equipment, batteries find innumerable applications. In this chapter a brief introduction about the battery chemistry and the important terminologies associated with the batteries will be highlighted. A battery stores chemical energy and converts it into electrical energy as and when required through an external circuit. A battery consists of one or more electrochemical cells. Although the terms battery and cell are often used interchangeably, cells are the building blocks of which batteries are constructed. Batteries consist of one or more cells that are electrically connected. The basic components of an electrolytic cell like a lead-acid cell are a *positive electrode,* a *negative electrode,* a *porous separator*, and an *electrolyte.* The schematic of a battery is shown in Figure 4. During cell operation, ions are created [3] and consumed at the two electrode/electrolyte interfaces by oxidation/reduction reactions. Both the electrodes must be electronically conducting in order to convey electrons to and from the reaction sites. The electrolyte, which can either be a solid or liquid chemical, has high conductivity for ions but not for electrons, because if the electrolyte conducts electrons then the battery will self-discharge. The electrolyte completes the internal circuit between the electrodes. The chemical reactions that are taking place in the two electrodes are summarized below:

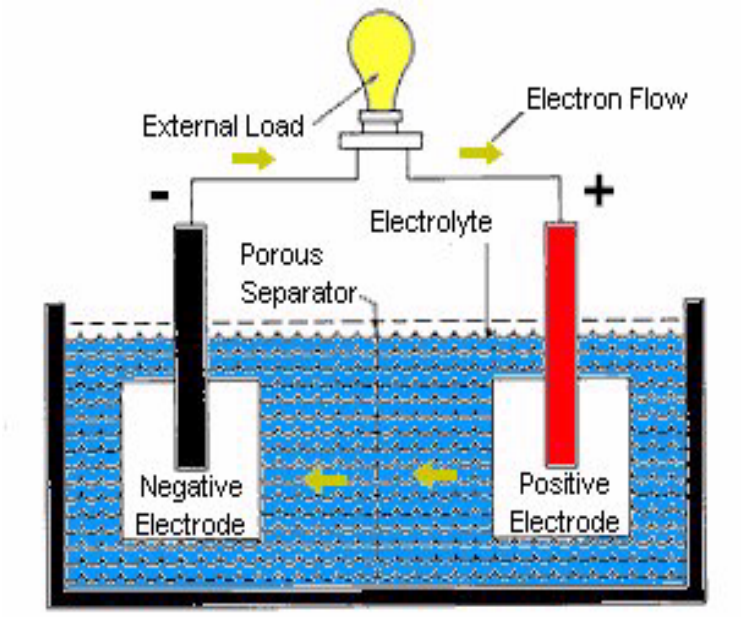


Figure 4. Battery and its components [Source: www.hepi.com]

Positive electrode reaction:

$$PbO_2 + SO_4^{-2} + 4H^+ + 2e^- \underset{Charge}{\overset{Discharge}{\rightleftharpoons}} PbSO_4 + 2H_2O\ (1.685V) \tag{2.3}$$

Negative electrode reaction:

$$Pb + SO_4^{-2} \underset{Charge}{\overset{Discharge}{\rightleftharpoons}} PbSO_4 + 2e^-\ (0.356V) \tag{2.4}$$

Overall reaction:

$$PbO_2 + Pb + 2H_2SO_4 \underset{Charge}{\overset{Discharge}{\rightleftharpoons}} 2PbSO_4 + 2H_2O\ (2.041V) \tag{2.5}$$

The electrode reactions show that the maximum open circuit voltage that can be developed by a single lead-acid cell is $2.041V$. It is a normal practice to connect these electrochemical cells in series or parallel to obtain the required battery voltage. For example, a

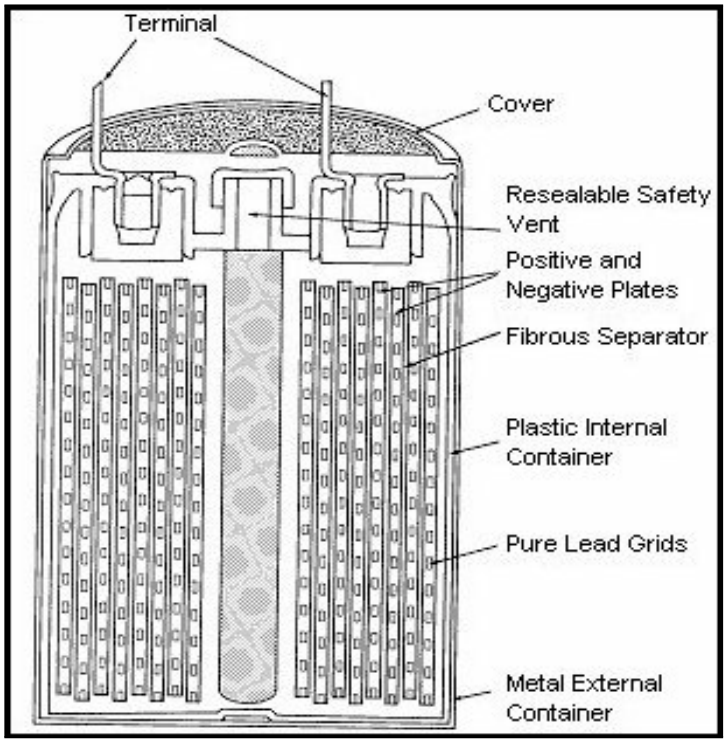


Figure 5. Cross-sectional view of a typical sealed lead-acid battery [Source: www.hepi.com]

$12V$ battery can be made using a series combinations of six cells each having a cell voltage of $2V$. A 16Ah capacity(Ampere-hour) Hawker Genesis [4] sealed lead-acid battery is used in this thesis for all the experiments. The cross-section of a typical sealed lead-acid battery is shown in Figure 5.

The sealed lead-acid battery [5] consists of positive and negative electrodes and their accompanying separators that are wound in a spiral pattern. The electrodes consist of pure lead grids pasted with mixtures of lead oxides. These oxides are converted to the proper active materials when the cell receives its first charge in a process called formation. The pure lead supporting grids allow the flexibility needed for winding the plate and also give

excellent corrosion resistance to prolong cell life. The separator consists of a fibrous glass material. The sealed-lead system has proven to provide high performance and long life in a clean, compact package and is widely used in HEV applications. In the following section the various battery parameters associated with the lead-acid battery is presented.

2.1 Battery parameters

There are several parameters associated with battery modeling [6], and these parameters are briefly explained below:

- *Internal Resistance*:
  - *Self-discharge resistance:* It is the resistance that is associated with the electrolysis of water at high voltage levels and slow leakage across the battery terminal at low voltage. This resistance is more temperature sensitive and is inversely proportional [6] to the temperature.
  - *Charge and Discharge resistance (R_c/R_d):* These resistances are associated with the electrolyte resistance, plate resistance, and fluid resistance; and these resistances vary during charging and discharging.
  - *Overcharge and Over discharge resistance:* These resistances are attributed largely to the electrolyte diffusion during over charging and over discharging.
- *Polarization Capacitance (C):* This is the capacitance due to the chemical diffusion within the battery and does not necessarily represent a purely electrical capacitance. It

depends on SOC, temperature and also the device design.

- *Discharge Type:*
  - *Continuous discharging:* In this case, the battery continuously delivers energy to the load which leads to a continuous drop in the battery capacity.
  - *Intermittent discharging:* In this case, the battery delivers energy to the load at regular or irregular intervals of time, as in HEVs where the energy is drawn by the motor for some period followed by the voltage recovery period.
- *Discharge Mode:*
  - *Constant load mode:* In this mode, the battery delivers energy to a constant load. The load current decreases proportional to the decrease in the battery terminal voltage, e.g. Electric Vehicle.
  - *Constant current mode:* In this mode, the battery supplies constant current to the load. This is achieved by continuously reducing the load resistance to match with the decreasing battery terminal voltage in order to maintain a constant current to the load.
  - *Constant power mode:* In this mode, the battery supplies constant electrical power to the load. The load current increases to compensate for the drop in voltage in order to maintain constant power to the load.
- *Rate of Charge and Discharge:* To extend service life of the battery, the rate of charge or discharge should not be too high. Also the frequency of charging and discharging cycles

affect the battery life significantly. The frequency of switching between charging and discharging is especially high in electric and hybrid electric vehicles which drastically reduces the life of the battery.

2.2 Various models available for battery modeling

There are many models available for battery modeling, and a few of them are mentioned here in this section. The merits and demerits of those models and the reason for choosing the modified Thevenin equivalent model in this thesis is also given.

2.2.1 Simple battery model

The most commonly used battery model is shown in Figure 6. It consists of an ideal battery with open-circuit voltage V_0, a constant equivalent internal resistance R_{int} and the terminal voltage represented by V_t. The terminal Voltage V_t can be obtained from the open circuit measurement, and R_{int} can be measured by connecting a load and measuring both the terminal voltage and current, at fully charged condition. While this model seems to be very simple, it does not take into consideration the varying nature of the internal resistance due to temperature, state of charge, and electrolytic concentration. This kind of model can only be used for certain circuit simulation, and it cannot be used for HEV or EV applications.

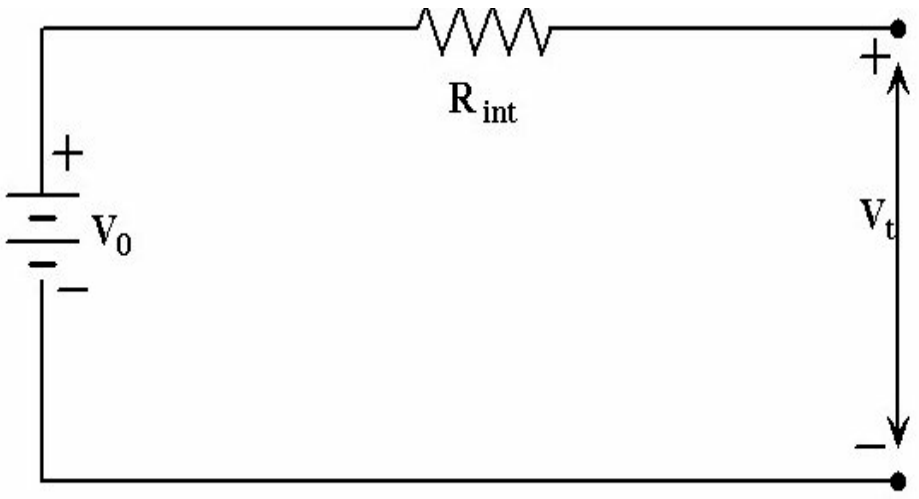


Figure 6. Simple battery model

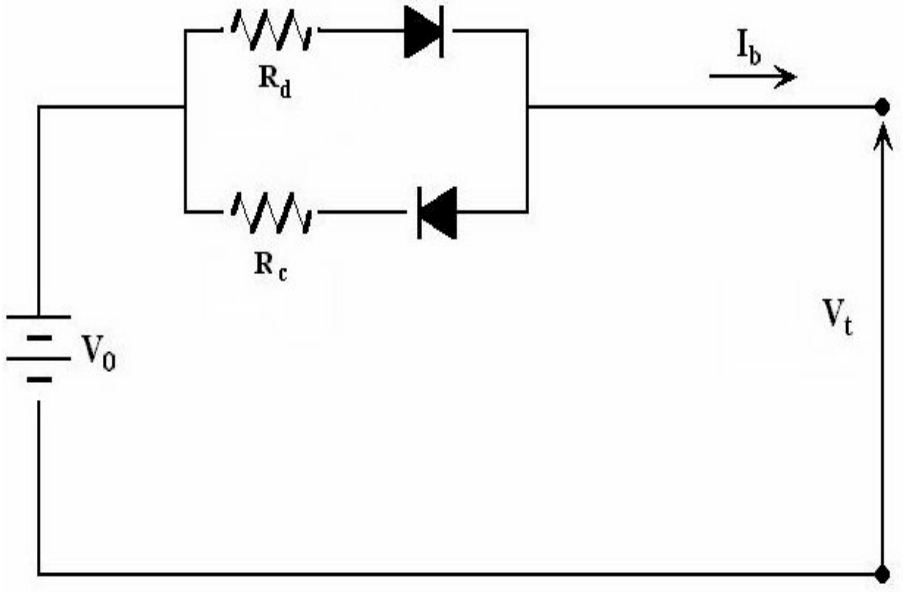


Figure 7. Thevenin battery model

2.2.2 *Resistive Thevenin battery model*

The resistive Thevenin battery model [1] is similar to the model described in section 2.2.1, but it assumes the following

- The electrodes are made of porous materials.
- The electrolytic resistance is constant throughout discharge.
- The discharge occurs at constant current.
- Polarization is a linear function of the active material current density.

The circuit diagram for resistive Thevenin battery model is shown in Figure 7. This model has two kinds of internal resistances, R_c and R_d, which are associated with the charging and discharging process of the battery, respectively. These two parameters (R_c

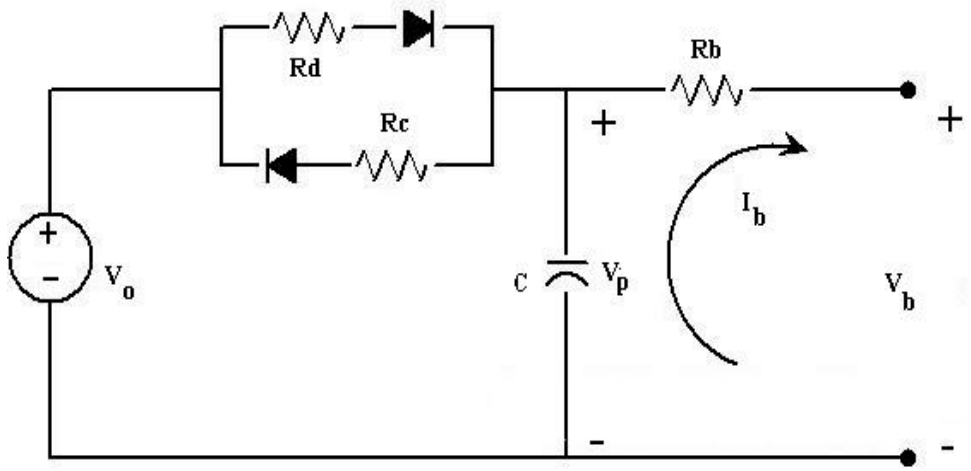


Figure 8. Modified Thevenin equivalent battery model

and R_d) model all forms of energy loss which includes electrical and non-electrical losses. The diodes, shown in Figure 7, implies that the during charging or discharging only one of the resistances R_c or R_d (which is in series with the forward biased diode) will be used because when one diode is forward biased the other will be reverse biased. These diodes are present only for modeling purposes only and have no physical significance in the battery. While this model is better than the previous model described in section 2.2.1, it does not account for the capacitance effect such as the transient current conditions occurring in the battery. Hence this model is non-dynamic in nature and is not suited for HEV or EV applications.

2.2.3 Modified Thevenin equivalent battery model

A simple dynamic battery model presented in [7] was considered by Farrell in [1] and this model is shown in Figure 8. The dynamic equations of the circuit model for discharg-

ing and charging are given by,

$$\dot{V}_p = \frac{dV_p}{dt} = -V_p\frac{1}{R_dC} + V_0\frac{1}{R_dC} - I_b\frac{1}{C}, \quad V_p \leq V_0 \tag{2.6}$$

$$\dot{V}_p = -V_p\frac{1}{R_cC} + V_0\frac{1}{R_cC} - I_b\frac{1}{C}, \quad V_p > V_0 \tag{2.7}$$

where

$$I_b = \frac{V_p - V_o}{R_b} \tag{2.8}$$

The direction of battery discharging current is considered to have positive sign throughout the thesis. In the special case when $R_b = 0$, then $V_p = V_0$, and the battery current is determined solely by the load resistance. The capacitance C represented in this figure is the polarization capacitance which is described in section 2.1. This particular circuit model is chosen for this thesis to determine the state of charge of the battery because of the following reasons:

- It accounts for the electrical and non-electrical energy losses, during charging and discharging processes of the battery, through the choice of the circuit parameters R_d and R_c.
- It takes care of the transient current conditions occurring in the HEV and EV operations by including the polarization capacitance C.
- It is dynamic in nature.
- The SOC of the battery can easily be calculated by Equation (1.1) as given in section 1.2.

- Overall it takes care of the resistance and capacitances not only due to electric phenomenon but also due to electrolysis of water in the battery and other effects due to temperature.
- Under no load conditions i.e. when $i_b = 0$, $V_b = V_p$ both of which converge exponentially toward V_0 with a time constant determined by R_dC (when previously being charged).

2.3 Mathematical equations of the modified Thevenin's equivalent model

In this section, the dynamic equations of the modified Thevenin's equivalent model, shown in Figure 6 is derived and a non-linear equation to represent the battery terminal voltage is obtained. After deriving the terminal voltage equation, a method to determine the open circuit voltage will be explained from which state of charge of the battery can be easily obtained.

The open circuit voltage, internal capacitor voltage and the terminal voltage are represented by V_o, V_p and V_b respectively. The charging, discharging and the internal resistance of the battery are represented by R_c, R_d, and R_b, respectively; and the polarization capacitance of the battery is represented by C. The current I_b is taken as positive if discharging and negative otherwise. The loop equations pertaining to the circuit model are

represented by Equation (2.9).

$$\begin{aligned} \dot{V_p} &= \frac{1}{C}\left(\left(\frac{V_o - V_p}{R_d}\right) - I_b\right) \\ V_b &= V_p - I_b R_b \end{aligned} \tag{2.9}$$

By defining the following state variables, a state space model of the battery can be formulated.

$$x_1 = V_p; x_2 = \frac{1}{R_d C}; x_3 = \frac{V_o}{R_d C}; x_4 = \frac{1}{C}; x_5 = R_b \tag{2.10}$$

A state space model of the above circuit, as given in [1], is slightly modified. The white noise processes in the system and measurement are taken to be zero $(w = 0, v = 0)$. Then the modified state space equations can be written as

$$\begin{aligned} \dot{x}_1 &= -x_1 x_2 + x_3 - I_b(t) x_4 \\ \dot{x}_2 &= 0 \\ \dot{x}_3 &= 0 \\ \dot{x}_4 &= 0 \\ \dot{x}_5 &= 0 \\ V_b &= x_1 - I_b(t) x_5 \end{aligned} \tag{2.11}$$

where

$$x(0) = (x_{10}, x_{20}, x_{30}, x_{40}, x_{50})^T \tag{2.12}$$

is unknown and $x_{10}, x_{20}, x_{30}, x_{40}, x_{50}$ are constants. The solution to the state equations are

given by

$$x_1(t) = \int_{t_0}^{t} e^{-x_{20}(t-\tau)}(x_{30} - I_b(\tau)x_{40})d\tau + x_{10}e^{-x_{20}(t-t_0)} \quad (2.13)$$

$$x_2(t) = x_{20} \quad (2.14)$$

$$x_3(t) = x_{30} \quad (2.15)$$

$$x_4(t) = x_{40} \quad (2.16)$$

$$x_5(t) = x_{50} \quad (2.17)$$

and the terminal battery voltage, $y(t)$, is given by

$$y(t) = \int_{t_0}^{t} e^{-x_{20}(t-\tau)}[x_{30} - I_b(\tau)x_{40}]d\tau + x_{10}e^{-x_{20}(t-t_0)} - I_b(t)x_{50} \quad (2.18)$$

In order to integrate this equation, it is easier to separate into simpler integrals. The integrals can be re-written in simpler integrals as

$$y(t) = \underbrace{\int_{t_0}^{t} x_{30}e^{-x_{20}(t-\tau)}d\tau}_{I_1} - \underbrace{\int_{t_0}^{t} x_{40}e^{-x_{20}(t-\tau)}I_b(\tau)d\tau}_{I_2} + x_{10}e^{-x_{20}(t-t_0)} - I_b(t)x_{50} \quad (2.19)$$

The value of integral I_1, after integration, is given by

$$I_1 = \frac{x_{30}}{x_{20}}(1 - e^{-x_{20}(t-t_0)}). \quad (2.20)$$

The battery current waveform is modeled as a quadratic equation which is linear in its parameters (a, b and c). Let the current profile be represented as the best fit to a quadratic as

$$I_b(t) = a + b(t - t_0) + c(t - t_0)^2 \quad (2.21)$$

$$= a + bt - bt_0 + ct^2 - 2ctt_0 + ct_0^2$$

The integral I_2 can be expanded as

$$\begin{aligned} I_2 &= x_{40}e^{-x_{20}t}\int_{t_0}^{t}(a+b\tau-bt_0+c\tau^2-2ct_0\tau+ct_0^2)e^{x_{20}\tau}d\tau \quad (2.22)\\ &= \underbrace{x_{40}e^{-x_{20}t}\int_{t_0}^{t}(a+b\tau)e^{x_{20}\tau}d\tau}_{I_3}+ \quad (2.23)\\ &\quad \underbrace{x_{40}e^{-x_{20}t}\int_{t_0}^{t}(-bt_0+c\tau^2-2ct_0\tau+ct_0^2)e^{x_{20}\tau}d\tau}_{I_4} \end{aligned}$$

The integral I_3 is given by

$$\begin{aligned} I_3 &= x_{40}e^{-x_{20}t}(\int_{t_0}^{t}ae^{x_{20}\tau}d\tau+\int_{t_0}^{t}b\tau e^{x_{20}\tau}d\tau) \quad (2.24)\\ &= x_{40}e^{-x_{20}t}\left(\frac{a}{x_{20}}(e^{x_{20}t}-e^{x_{20}t_0})+\frac{b}{x_{20}}(te^{x_{20}t}-t_0e^{x_{20}t_0})-\frac{b}{x_{20}^2}(e^{x_{20}t}-e^{x_{20}t_0})\right)\\ I_3 &= a\frac{x_{40}}{x_{20}}(1-e^{-x_{20}(t-t_0)})+b\frac{x_{40}}{x_{20}}(t-t_0e^{-x_{20}(t-t_0)})-b\frac{x_{40}}{x_{20}^2}(1-e^{-x_{20}(t-t_0)}) \end{aligned}$$

The integral I_4 is found to be

$$\begin{aligned} I_4 &= x_{40}e^{-x_{20}t}\left(\int_{t_0}^{t}(-bt_0+ct_0^2)e^{x_{20}\tau}d\tau+\int_{t_0}^{t}(c\tau^2-2ct_0\tau)e^{x_{20}\tau}d\tau\right) \quad (2.25)\\ &= x_{40}e^{-x_{20}t}(-bt_0+ct_0^2)\left(\frac{1}{x_{20}}(e^{x_{20}t}-e^{x_{20}t_0})\right)\\ &\quad +x_{40}e^{-x_{20}t}\left(\frac{c}{x_{20}}(t^2e^{x_{20}t}-t_0^2e^{x_{20}t_0})-\frac{2c}{x_{20}}\left(\frac{te^{x_{20}t}-t_0e^{x_{20}t_0}}{x_{20}}-\frac{e^{x_{20}t}-e^{x_{20}t_0}}{x_{20}^2}\right)\right)\\ &\quad -x_{40}e^{-x_{20}t}\left(2ct_0\left(\frac{te^{x_{20}t}-t_0e^{x_{20}t_0}}{x_{20}}-\frac{e^{x_{20}t}-e^{x_{20}t_0}}{x_{20}^2}\right)\right) \end{aligned}$$

The following notations are employed to simplify the equations

$$c_1=x_{10};c_2=x_{20};c_3=\frac{x_{30}}{x_{20}};c_4=\frac{x_{40}}{x_{20}};c_5=x_{50};t_k=t-t_0 \quad (2.26)$$

The integrals I_1, I_3 and I_4, after using the notations, are then

$$I_1 = c_3(1 - e^{-c_2 t_k}) \tag{2.27}$$

$$I_3 = ac_4(1 - e^{-c_2 t_k}) + bc_4(t - t_0 e^{-c_2 t_k}) - b\frac{c_4}{c_2}(1 - e^{-c_2 t_k}) \tag{2.28}$$

$$\begin{aligned} I_4 = {} & (-bc_4 t_0 + cc_4 t_0^2)(1 - e^{-c_2 t_k}) + cc_4(t^2 - t_0^2 e^{-c_2 t_k}) \\ & -2c\frac{c_4}{c_2}(t - t_0 e^{-c_2 t_k}) + \frac{2cc_4}{c_2^2}(1 - e^{-c_2 t_k}) - 2cc_4 t_0(t - t_0 e^{-c_2 t_k}) \\ & +\frac{2cc_4 t_0}{c_2}(1 - e^{-c_2 t_k}) \end{aligned} \tag{2.29}$$

Now combining $I_{1,}I_{3,}I_4$ and the other parts of Equation (2.19), we get

$$\begin{aligned} y(t) = {} & c_3(1 - e^{-c_2 t_k}) - ac_4(1 - e^{-c_2 t_k}) + bc_4(t - t_0 e^{-c_2 t_k}) \\ & -b\frac{c_4}{c_2}(1 - e^{-c_2 t_k}) + (-bc_4 t_0 + cc_4 t_0^2)(1 - e^{-c_2 t_k}) + cc_4(t^2 - t_0^2 e^{-c_2 t_k}) \\ & -2c\frac{c_4}{c_2}(t - t_0 e^{-c_2 t_k}) + \frac{2cc_4}{c_2^2}(1 - e^{-c_2 t_k}) - 2cc_4 t_0(t - t_0 e^{-c_2 t_k}) \\ & +\frac{2cc_4 t_0}{c_2}(1 - e^{-c_2 t_k}) + c_1 e^{-c_2 t_k} - c_5\left(a + b(t - t_0) + c(t^2 - 2tt_0 + t_0^2)\right) \end{aligned} \tag{2.30}$$

After collecting similar terms together, Equation (2.30) can be rewritten as

$$\begin{aligned} y(t) = {} & c_3 - a(c_4 + c_5) + (b - 2\frac{c}{c_2})\frac{c_4}{c_2} \\ & -\left(b(c_4 + c_5) - 2c\frac{c_4}{c_2}\right)(t - t_0) - c(c_4 + c_5)(t - t_0)^2 \\ & +\left(c_1 - c_3 + ac_4 - b\frac{c_4}{c_2} + 2\frac{c}{c_2}\frac{c_4}{c_2}\right)e^{-c_2(t - t_0)} \end{aligned} \tag{2.31}$$

In order to give a simple structure to the terminal battery voltage, $y(t)$, the following q

parameters are defined.

$$q_1 \triangleq c_3 - a(c_4 + c_5) + (b - 2\frac{c}{c_2})\frac{c_4}{c_2} \tag{2.32}$$

$$q_2 \triangleq c_2 \tag{2.33}$$

$$q_3 \triangleq -\left(b(c_4 + c_5) - 2c\frac{c_4}{c_2}\right) \tag{2.34}$$

$$q_4 \triangleq -c(c_4 + c_5) \tag{2.35}$$

$$q_5 \triangleq c_1 - c_3 + ac_4 - (b - 2\frac{c}{c_2})\frac{c_4}{c_2} \tag{2.36}$$

With the help of q_i parameters, the terminal battery voltage (Equation (2.31)) can be represented as

$$y(t) = q_1 + q_3(t - t_0) + q_4(t - t_0)^2 + q_5 e^{-q_2(t-t_0)} \tag{2.37}$$

Choice of $I_b(t)$:

At this juncture the reason for choosing $I_b(t) = a + b(t - t_0) + c(t - t_0)^2$ has to be explained in order to appreciate the equations derived so far. The simplest choice of $I_b(t)$ would be a linear fit which can be represented as $I_b(t) = a + b(t - t_0)$.In this case the value of $c = 0$ and so the Equations (2.32), (2.34), (2.35) and (2.36), can be written as

$$\begin{aligned} q_1 &= c_3 - a(c_4 + c_5) + b\frac{c_4}{c_2} \\ q_2 &= c_2 \\ q_3 &= -b(c_4 + c_5) \\ q_4 &= 0 \\ q_5 &= c_1 - c_3 + ac_4 - b\frac{c_4}{c_2} \end{aligned} \tag{2.38}$$

In the Equation (2.38), the number of unknowns (c_1, c_2, c_3, c_4, c_5) are greater than the number of equations and it seem that one cannot solve c_3. By adding the term '$c(t-t_0)^2$' in $I_b(t)$, this problem is eliminated. That is, there must be sufficient variation in the current $I_b(t)$ in order to identify the open circuit voltage $V_{oc} = c_3$.

By the definition in Equation (2.26), the physical meaning of the c_i parameters are enumerated for reference.

$$\begin{aligned} c_1 &= V_p(t_0) \text{ (Capacitor Voltage)} \\ c_2 &= \frac{1}{R_d C} \\ c_3 &= V_{oc} \text{ (Open circuit voltage)} \\ c_4 &= R_d \\ c_5 &= R_b \end{aligned} \tag{2.39}$$

The important c_i parameters can be written in terms of q_i parameters as shown below

$$\begin{aligned} c_2 &= q_2 \\ c_4 + c_5 &= -\frac{q_4}{c} \\ \frac{c_4}{c_2} &= \frac{1}{2c}\left(q_3 - b(\frac{q_4}{c})\right) \\ c_3 &= q_1 + a(-\frac{q_4}{c}) - \frac{1}{2c}\left(q_3 - b(\frac{q_4}{c})\right)\left(b - 2\frac{c}{q_2}\right) \end{aligned} \tag{2.40}$$

So far the equation to represent the terminal battery voltage has been derived. The next step is to determine the open circuit voltage of the battery by making use of the derived equation. The only measurements that are obtained from the battery are the battery terminal voltage, $y(t)$,and the battery current, $I_b(t)$. The OPTIMIZATION TOOLBOX from

MATLAB is used to find the estimated terminal voltage, $\hat{y}(t)$,based on the q's in Equation (2.37). A squared error function which is given by

$$F(t) = \int_{t_0}^{t} [y(t) - \widehat{y}(t)]^2 dt \tag{2.41}$$

where $\hat{y}(t)$ is given by

$$\widehat{y}(t) \;=\; \widehat{q_1} + \widehat{q_3}(t - t_0) + \widehat{q_4}(t - t_0)^2 + \widehat{q_5} e^{-\widehat{q_2}(t-t_0)} \tag{2.42}$$

($\widehat{q}$'s are the estimated values)

is used to compare the measured and estimated terminal battery voltages. The objective is to minimize this error function, Equation (2.41), so that the $\hat{q}$'s are a good estimate of the measured terminal voltage.

Equation (2.41) is the error between the actual terminal voltage, $y(t)$, and the estimated terminal voltage, $\widehat{y}(t)$, over the period given by $T = t - t_0$, and the objective here is to minimize the error. By substituting Equation (2.42) in Equation (2.41), we obtain the following

$$F(\widehat{y}(t), \widehat{q_1}, \widehat{q_2}, \widehat{q_3}, \widehat{q_4}, \widehat{q_5}) = \int_{t_0}^{t} (y(t) - (\widehat{q_1} + \widehat{q_3}(t-t_0) + \widehat{q_4}(t-t_0)^2 + \widehat{q_5} e^{-\widehat{q_2}(t-t_0)}))^2 dt \tag{2.43}$$

If the objective function given by Equation (2.43) is digitized, then we get the following equation

$$F = \sum_{k=0}^{N} (y(t_k) - (\widehat{q_1} + \widehat{q_3}(t - t_0) + \widehat{q_4}(t - t_0)^2 + \widehat{q_5} e^{-\widehat{q_2}(t-t_0)}))^2 \Delta t \tag{2.44}$$

where $\Delta t = T/N$ and $t_k = k\Delta t$.

The values of $\widehat{q_i}$'s that minimizes the error function, F, are obtained from the OPTIMIZATION TOOLBOX from which the open circuit voltage parameter is identified and

hence the state of charge of the battery.

2.4 V_{OC} estimation strategy

In order to obtain the open circuit voltage of the battery, the $\hat{q}_i$'s are used. The open circuit voltage is given by c_3, and it is given by

$$c_3 = q_1 + a(c_4 + c_5) - (b - 2\frac{c}{c_2})\frac{c_4}{c_2} \quad (2.45)$$

$$(c_4 + c_5) = -\frac{q_4}{c} \quad (2.46)$$

$$\frac{c_4}{c_2} = \frac{1}{2c}(q_3 - b\frac{q_4}{c}) \quad (2.47)$$

$$c_2 = q_2 \quad (2.48)$$

The a, b and c parameters are obtained from the measured current by least square method. The battery discharge current waveform used in simulation and the experiments is shown in Figure 9. In the figure, the a, b, and c parameters are different for each of the segments of the waveform, particularly when $I_b(t) = 0$ (e.g. $t = 200 - 300\,\mathrm{sec}\,s$), the parameters are $a = 0, b = 0$ and $c = 0$. In such cases it will be difficult to use Equation (2.46) and Equation (2.47), because the parameter c occurs in the denominator which makes those equations go to infinity. Therefore, some reasonable assumptions are made to estimate the open circuit voltage under such special cases. In the normal case, the open circuit voltage is estimated with the $q_i's$ as per Equation (2.45). The open circuit voltage is represented as

$$V_{oc} = c_3 = q_1 + a(-\frac{q_4}{c}) - (b - 2\frac{c}{c_2})\left(\frac{1}{2c}(q_3 - b\frac{q_4}{c})\right) \quad (2.49)$$

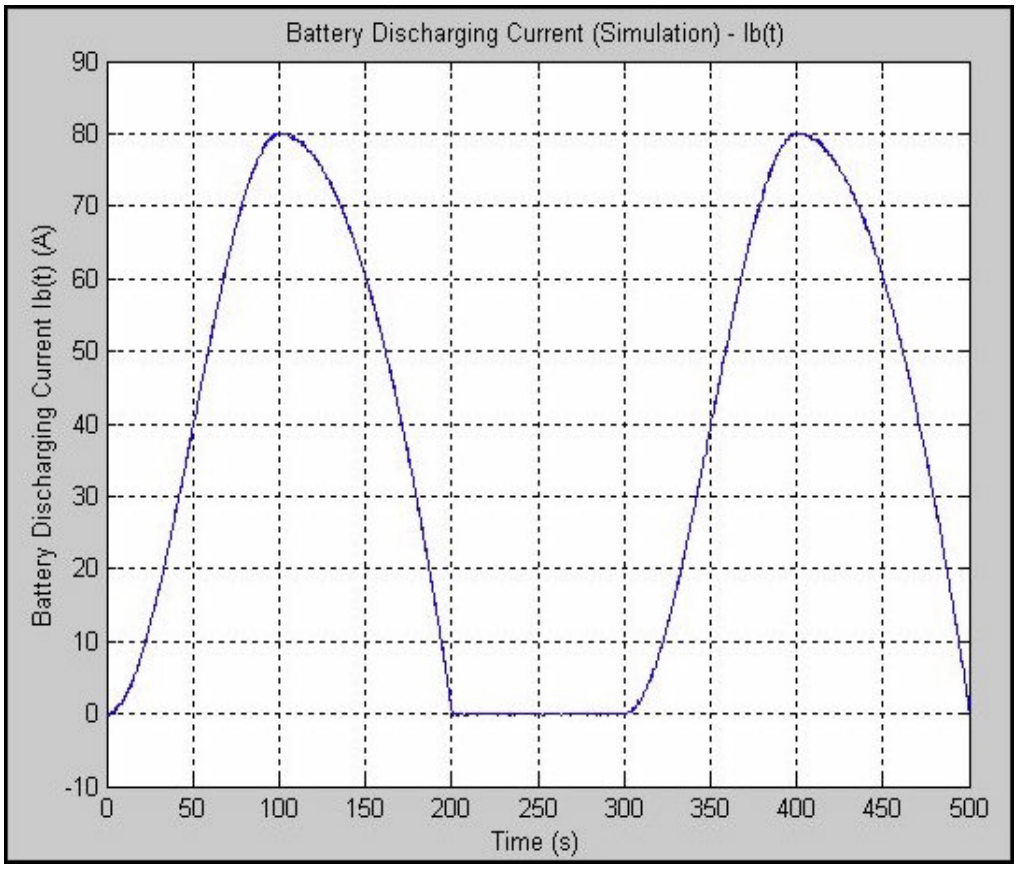


Figure 9. Battery discharging current Ib(t) used in simulation

Thus V_{OC} of the battery can be estimated with the knowledge of q_1, q_2, q_3, q_4, a, b and c. The next section throws light on the state of charge estimation of the battery.

2.5 SOC estimation strategy

State of charge of the battery is the by-product of following the procedures to estimated V_{OC} as mentioned in previous section. Once the V_{OC} is estimated then it is very easy to find the SOC of the battery with the help of Equation (1.1), which is given by

$$SOC(\%) = S(t) = \frac{v_{oc}(t) - b}{a} \tag{2.50}$$

The value of a and b parameters can be found experimentally when the battery is charged fully ($SOC = 100\%$) and when the battery charge is drained completely ($SOC = 0\%$), respectively. Then the SOC of the battery can be easily determined knowing the V_{OC} of the battery at any given instant.

2.6 Summary

In this chapter a battery model, modified Thevenin model, was considered for battery SOC estimation. The terminal battery voltage equation was derived which is non-linear in nature. Then the method to estimate the V_{OC} under various conditions are mentioned. The SOC of the battery can then be estimated knowing the V_{OC} of the battery.

Chapter 3
Simulation of the battery model using MATLAB

3.1 Simulation methods

To implement the SOC algorithm many methods were identified and analyzed. Few methods that were analyzed for implementing the SOC algorithm are described in this section. While one method was based on systems theory and observability Gramian [8] the other was based on using the linear and grid (exhaustive) search techniques using MATLAB's OPTIMIZATION TOOLBOX.

3.1.1 Minimization Techniques

In this method, the objective is to minimize the error function, as given below, over a small time period T. The objective function to be minimized is given by the following equation

$$\begin{aligned} F &= \sum_{k=0}^{N} (y(t_k) - \hat{y}(t_k))^2 \Delta t \qquad (3.51) \\ &= \sum_{k=0}^{N} (y(k) - (\hat{q}_1 + \hat{q}_3(t_k - t_0) + \hat{q}_4(t_k - t_0)^2 + \hat{q}_5 e^{-\hat{q}_2(t_k - t_0)}))^2 \Delta t \\ \text{where } \Delta t &= T/N, t_k = k\Delta t \text{ and } \widehat{q}_{i,i=1,2,3,4,5} \text{ are the estimated values of } \widehat{y}(t_k) \end{aligned}$$

The theory behind this method is already explained in section 2.3. Though there are different ways to obtain the minimum value of the function F, two methods are chosen for

practical implementation of this approach and are described below.

Optimization method using MATLAB *Toolbox*

In this method, the OPTIMIZATION TOOLBOX from MATLAB is utilized to find the optimum values of $\hat{q}_i$'s so that the reconstructed $\hat{y}(t_k)$ closely matches $y(t_k)$. The function $fmincon$ (*constrained minimization of objective function*) was used which basically minimizes the objective function, F, based on the initial value, lower and upper bound conditions placed on the $\hat{q}_i$ variables. Once the q_i variables are found then the open circuit voltage, V_{OC}, can easily be determined as described in section2.4 and the state of charge of the battery can also be estimated.

Limitations of the MATLAB *Toolbox*

This method is an ideal candidate for SOC estimation if not for the limitations that are discussed here. The OPTIMIZATION TOOLBOX finds only the *local* minimum of the objective function and not the *global* minimum. The implication of this statement is that when different *initial value conditions* are given to the function ($fmincon$) then the optimum value ($\hat{q}_i$'s) that are nearer to the initial values are returned. But in the real world, $\hat{q}_i$'s that globally minimizes the objective function are required hence this is a serious limitation of the OPTIMIZATION TOOLBOX.

Another limitation is the selection of the time period T, to determine the $\hat{q}_i$ variables. As mentioned before, the term '$\hat{q}_5 e^{-\hat{q}_2(t_k - t_0)}$' decays out within few seconds and so the

toolbox has difficulty in identifying the $\hat{q}_2$ and $\hat{q}_5$ parameters.

One way to overcome this difficulty was to differentiate $y(t)$ which results in the following equation,

$$\dot{y}(t) = q_3 + 2q_4(t - t_0) - q_2 q_5 e^{-q_2(t-t_0)} \tag{3.52}$$

By doing this alteration the toolbox could get the value of q_3 but not the values of q_2 ,q_4 and q_5 parameters. One of the important reason for the failure of this particular step is that the differentiated value of $y(t)$ is prone to high frequency noise. In real time data the noise content will be more in addition to the measurement noise. Also the real battery terminal voltage was constant for certain time intervals as shown in Figure 10. Then the differentiated value of $y(t), \dot{y}(t) = 0$, in those intervals. In such case the toolbox could only make all the parameters to zero to yield the minimum value of the objective function. Hence this method could not yield satisfactory results.

Grid search method

This is the most straight forward way of finding the global minimum of the objective function. In this method each of the q_i parameters are varied from their lower bounds to their upper bounds in some incremental steps to do an exhaustive search to find the minimum value of the error function. The particular set of q_i values that gives the lowest value for the error function is then identified. The incremental step size determines the time taken to compute the whole process and find the overall minimum. This method will find the global minimum of the objective function. Once the q_i are identified then, using

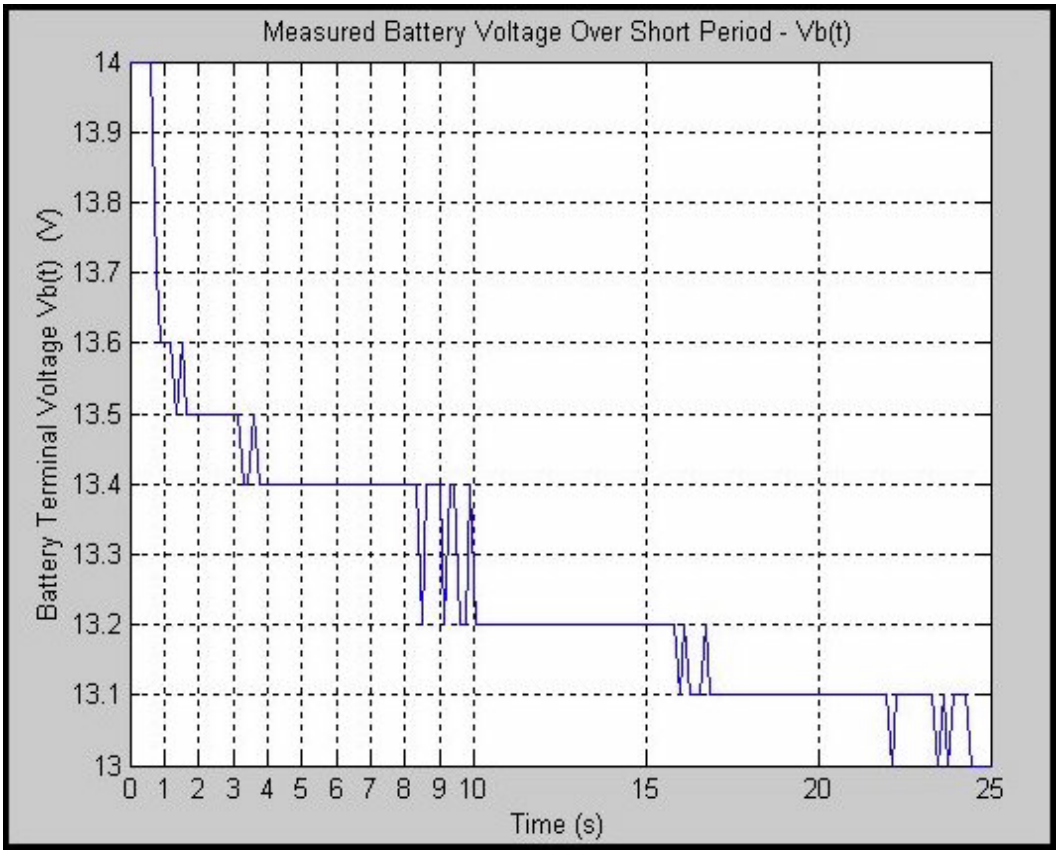


Figure 10. Real battery terminal voltage Vb(t)

Equation (2.49), V_{OC} and hence the SOC are easily determined.

Limitations of the Grid search method

The major shortcoming of this method and why it is not a preferred method is that it is very time consuming because it performs an exhaustive search to find the minimum value of the error function. This method is not feasible as a direct application but it may be combined with the other methods to yield a satisfactory result.

A combination of optimization and grid search methods

As mentioned earlier grid search techniques alone is not preferred but when it is combined with,say Optimization techniques, computation time is reduced. Another modification made is that noting the fact that the magnitude of q_4 was approximately 10 times smaller compared to the the other parameters, it could be removed from the Equation (3.52). The value of q_3 is obtained through OPTIMIZATION TOOLBOX as mentioned earlier and then the other two parameters are identified by grid search techniques.

3.1.2 System Theory Approach - Observability Gramian Method

In this section the system theory principle applied to get the open circuit voltage of the battery is explained. The system given in Equation (2.11) is a *nonlinear time-varying* system. If the initial condition (parameter) $x_{20} = c_{20}$ in Equation (2.11) is known, then the system equations may be rewritten as a (reduced-order) *linear time-varying* system given

by

$$\frac{dx}{dt} = \begin{bmatrix} -c_{20} & 1 & -I_b(t) & 0 \\ 0 & 0 & 0 & 0 \\ 0 & 0 & 0 & 0 \\ 0 & 0 & 0 & 0 \end{bmatrix} x \tag{3.53}$$

and

$$y = \begin{bmatrix} 1 & 0 & 0 & -I_b(t) \end{bmatrix} x$$

$$x \triangleq (x_1, x_3, x_4, x_5)$$

More compactly, we have

$$\begin{aligned} dx/dt &= A(t, x_{20})x(t),\ x(t_0) = x_0 = (x_{10}, x_{30}, x_{40}, x_{50}) \\ y(t) &= C(t)x(t) \end{aligned} \tag{3.54}$$

with the obvious definitions for $A(t, x_{20})$ and $C(t)$. If this system satisfies certain observability criteria, then one can accurately estimate the $V_{oc} = x_{30}/x_{20}$ by computing the observability Gramian of the system. This is now outlined below.

Observability deals with the influence of the state vector on the output, and does not involve the effect of a known input signal. By definition [8], the unforced linear state equation, Equation (3.54) is called *observable* on $[t_0, t_f]$ if any initial state x_0 is uniquely determined by its corresponding response $y(t)$, for $t\ \epsilon\ [t_0, t_f]$. The assumptions made here in this case are that the values given by $x_0 = (x_{10}, x_{30}, x_{40}, x_{50})$ are constants over the period $[t_0, t_f]$. This is a reasonable assumption if actual system parameters vary slowly. The parameter of concern here is the ratio $x_{30}/x_{20} = V_{oc}$. The state transition matrix of

the system defined by Equation (3.54) is defined as the solution to

$$\frac{d\Phi(t,t_0,x_{20})}{dt} = A(t,x_{20})\Phi(t,t_0,x_{20}) \tag{3.55}$$

and

$$\Phi(t_0,t_0,x_{20}) = I_{n\times n} \tag{3.56}$$

In order to calculate x_0 the following condition has to be met. The linear state equation given by Equation (3.54) is observable on $[t_0,t_f]$ if and only if the $n \times n$ matrix M given by Equation (3.57), is invertible.

$$M(t_0,t_f) \triangleq \int_{t_0}^{t_f} \Phi^T(t,t_0)C^T(t)C(t)\Phi(t,t_0)dt \tag{3.57}$$

If M is invertible then the initial states represented by x_0 can be easily found using Equation

$$\int_{t_0}^{t_f} \Phi^T(t,t_0,x_{20})C^T(t)y(t)dt = M(t_0,t_f)x_0$$

and therefore

$$x_0 = M^{-1}(t_o,t_f)\int_{t_0}^{t_f} \Phi^T(t,t_0,x_{20})C^T(t)y(t)dt \tag{3.58}$$

By referring to Equation (2.11), the following matrices can be easily identified. Another significant assumption made in this method is that the state variable $x_2(=\frac{1}{R_dC}=c_{20}(say))$ is known a priory. After eliminating x_2 from the state equations, based on the assumption,

we get the following matrices,

$$A(t) = \begin{bmatrix} -c_{20} & 1 & -I_b(t) & 0 \\ 0 & 0 & 0 & 0 \\ 0 & 0 & 0 & 0 \\ 0 & 0 & 0 & 0 \end{bmatrix} \tag{3.59}$$

and

$$C(t) = \begin{bmatrix} 1 & 0 & 0 & -I_b(t) \end{bmatrix} \tag{3.60}$$

Let the state transition matrix $\Phi(t, t_0, x_{20})$ be represented as

$$\Phi(t, t_0, x_{20}) = \begin{bmatrix} \Phi_{11} & \Phi_{12} & \Phi_{13} & \Phi_{14} \\ \Phi_{21} & \Phi_{22} & \Phi_{23} & \Phi_{24} \\ \Phi_{31} & \Phi_{32} & \Phi_{33} & \Phi_{34} \\ \Phi_{41} & \Phi_{42} & \Phi_{43} & \Phi_{44} \end{bmatrix} \tag{3.61}$$

The properties mentioned below in Equation (3.62) is utilized to evaluate the state transition matrix as given below,

$$\frac{d\Phi(t, t_0, x_{20})}{dt} = \begin{bmatrix} d\Phi_{11}/dt & d\Phi_{12}/dt & d\Phi_{13}/dt & d\Phi_{14}/dt \\ 0 & 0 & 0 & 0 \\ 0 & 0 & 0 & 0 \\ 0 & 0 & 0 & 0 \end{bmatrix} \tag{3.62}$$

where

$$\frac{d\Phi_{11}}{dt} = -\Phi_{11} c_{20} \tag{3.63}$$

$$\frac{d\Phi_{12}}{dt} = -\Phi_{12} c_{20} + 1 \tag{3.64}$$

$$\frac{d\Phi_{13}}{dt} = -\Phi_{13} c_{20} - I_b(t) \tag{3.65}$$

$$\frac{d\Phi_{14}}{dt} \equiv 0 \tag{3.66}$$

The Equations (3.63), (3.64), (3.65), and (3.66) can be implemented in SIMULINK and the values of $\Phi(t, t_0, x_{20})$ can be obtained. This is shown in Figure 11. The next step after getting $\Phi(t, t_0)$ is to compute the *observability Gramian (M)* and to check if it is invertible or in other words to verify if M is of full rank In order to determine M the

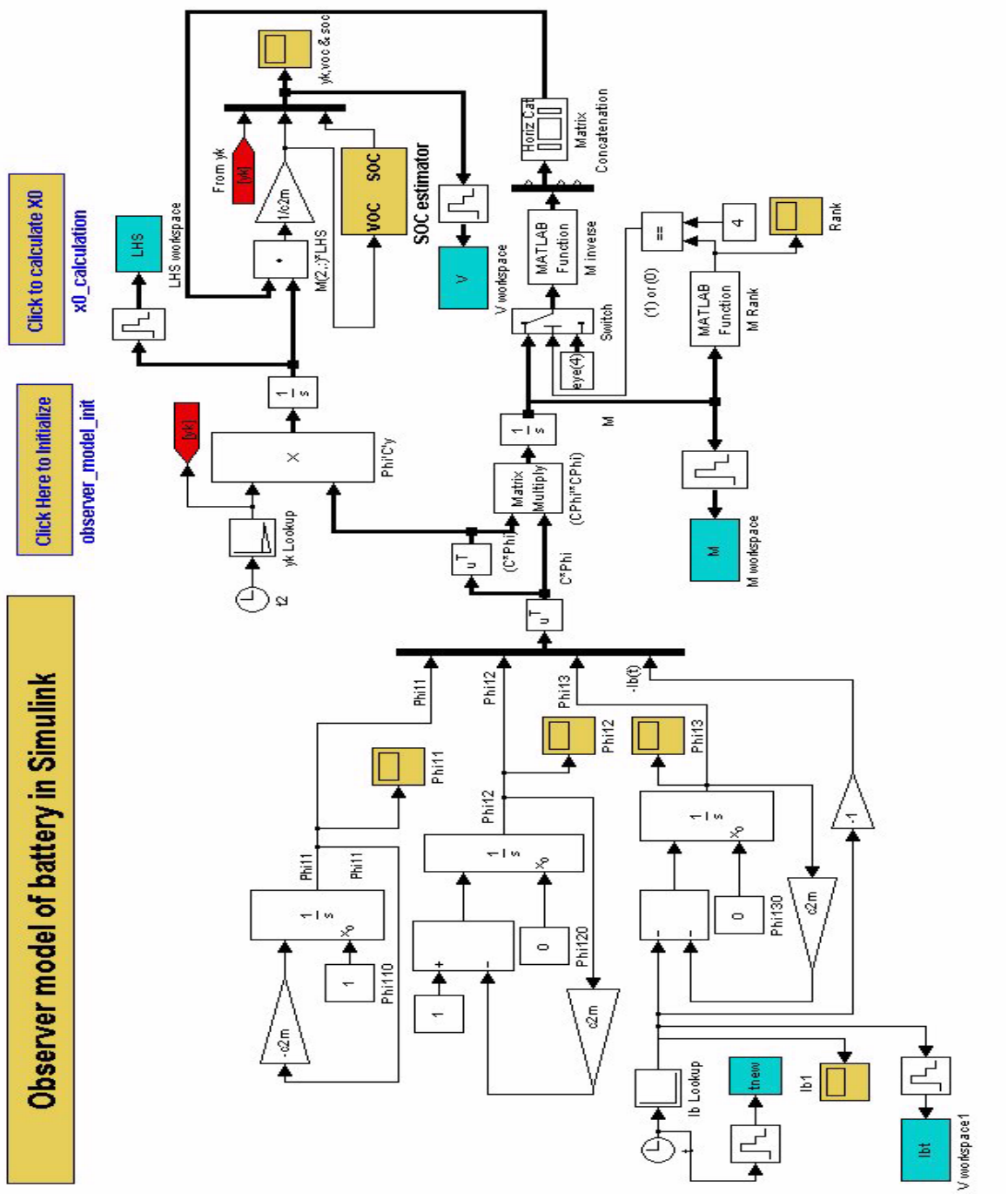


Figure 11. Simulink model of the battery

following matrices needs to be computed,

$$C(t) * \Phi(t, to) = \begin{bmatrix} \Phi_{11} & \Phi_{12} & \Phi_{13} & -I_b(t) \end{bmatrix} \tag{3.67}$$

and their transpose is given by

$$\Phi^T(t, t_0) * C(t) = \begin{bmatrix} \Phi_{11} \\ \Phi_{12} \\ \Phi_{13} \\ -I_b(t) \end{bmatrix} \tag{3.68}$$

The product of Equations (3.67) and (3.68) is then

$$\Phi^T(t, t_0) C^T(t) C(t) \Phi(t, t_0) = \begin{bmatrix} \Phi_{11}^2 & \Phi_{11}\Phi_{12} & \Phi_{11}\Phi_{13} & -\Phi_{11} I_b(t) \\ \Phi_{12}\Phi_{11} & \Phi_{12}^2 & \Phi_{12}\Phi_{13} & -\Phi_{12} I_b(t) \\ \Phi_{13}\Phi_{11} & \Phi_{13}\Phi_{12} & \Phi_{13}^2 & -\Phi_{13} I_b(t) \\ -I_b(t)\Phi_{11} & -I_b(t)\Phi_{12} & -I_b(t)\Phi_{13} & I_b^2(t) \end{bmatrix} \tag{3.69}$$

The observability Gramian M is then found by using the Equation (3.57), by integrating the products within the integral over a small segment of time $[t_0, t_f]$. Substituting Equation (3.69) in Equation (3.57), we get

$$M(t_0, t_f) = \int_{t_0}^{t_f} \begin{bmatrix} \Phi_{11}^2 & \Phi_{11}\Phi_{12} & \Phi_{11}\Phi_{13} & -\Phi_{11} I_b(t) \\ \Phi_{12}\Phi_{11} & \Phi_{12}^2 & \Phi_{12}\Phi_{13} & -\Phi_{12} I_b(t) \\ \Phi_{13}\Phi_{11} & \Phi_{13}\Phi_{12} & \Phi_{13}^2 & -\Phi_{13} I_b(t) \\ -I_b(t)\Phi_{11} & -I_b(t)\Phi_{12} & -I_b(t)\Phi_{13} & I_b^2(t) \end{bmatrix} dt \tag{3.70}$$

where the values of Φ_{ij}'s are given by

$$\Phi_{11}(t, t_0, x_{20}) = e^{-c_2(t-t_0)} \tag{3.71}$$

$$\Phi_{12}(t, t_0, x_{20}) = \frac{1}{c_2}(1 - e^{-c_2(t-t_0)}) \tag{3.72}$$

$$\begin{aligned} \Phi_{13}(t, t_0, x_{20}) &= -\int_{t_0}^{t} e^{-c_2(t-\tau)} I_b(\tau) d\tau \text{ where } Ib(t) = a + b(t-t_0) + c(t-t_0)^2 \\ &= \left(\frac{2c - bc_2 + ac_2^2}{c_2^3}\right) e^{-c_2(t-t_0)} \\ &\quad -\frac{1}{c_2^3}\left(2c - bc_2 + ac_2^2 - 2cc_2(t-t_0) + bc_2^2(t-t_0) + cc_2^2(t-t_0)^2\right) \end{aligned} \tag{3.73}$$

$$\Phi_{14}(t, t_0, x_{20}) \equiv 0 \tag{3.74}$$

The analytical evaluation of the observability Gramian M is very tedious and cumbersome, hence it is numerically integrated in MATLAB. If the rank of the matrix M is full (or $rank = 4$, in this case) then $M^{-1}$is computed. The value of battery terminal voltage $y(t)$, and battery current $I_b(t)$, measured with the help of ABC-150 (described in section 4.1), are used in MATLAB. Then using the Equation (3.58), the initial states x_0 are identified from which the V_{oc} and hence the SOC is estimated. This method yield results that are comparable to the actual experimental values.

Advantages of observability Gramian method

The requirement for the Gramian method to work are as follows:

- A priory knowledge of $x_{20} = 1/R_dC$ to identify $V_{OC} = x_{30}/x_{20}$.
- Gramian M should be invertible.

The matrix M is invertible after a fraction of seconds and the initial states x_0 could easily be found. In the earliest part of the thesis it has been mentioned that $q_2 = c_2 = x_2 = 1/R_dC$, was a critical parameter in finding the V_{OC}. The value of the ratio x_{30}/x_{20}, over the limit given by Equation (3.75), is found to be independent of x_{20} and this is proved my rigorous mathematical calculation using MATHEMATICA, a software for mathematical computations, and is presented in the appendix.

$$\lim_{(t_f - t_0) -> \infty} \left(\frac{x_{30}}{x_{20}} \right) = \lim_{(t_f - t_0) -> \infty} \begin{pmatrix} \frac{1}{x_{20}} \begin{bmatrix} 0 & 1 & 0 & 0 \end{bmatrix} M^{-1}(t, t_0, x_{20}) \\ \int_{t_0}^{t_f} \Phi^T(t, t_0, x_{20}) C^T(t) y(t) dt \end{pmatrix} \tag{3.75}$$

Thus, by the above proof, we can estimate the V_{OC} of the battery even by assuming an arbitrary value of $x_{20} = c_{20}$. This is an important advantage of using the Gramian method.

3.2 Simulation procedure

There are various modules in MATLAB and they interact with each other very elegantly. This interaction can be illustrated with the help of Figure 12. SIMULINK, as an entity can accept information directly from the user and can also access the resources from the MATLAB workspace. The user has full command over the entire MATLAB environment.

There is a two step process associated with battery simulations. First, the simulation is completed in the SIMULINKand the results are exported to the MATLAB workspace. The next step is to invoke the OPTIMIZATION TOOLBOX through the MATLAB program editor. The OPTIMIZATION TOOLBOX gets the data from the MATLAB workspace and executes the specified functions and return the results to the MATLAB workspace. The user can then access the workspace to gather the results and analyze them. The subsequent sections briefly explains the role of SIMULINK and OPTIMIZATION TOOLBOX in the battery simulations.

3.3 Simulation setup in SIMULINK

The battery model was simulated with the help of SIMULINK in MATLAB [9], which is a powerful tool for engineers to perform and analyze simulations. SIMULINK is a software package that enables engineers to model, simulate, and analyze systems whose outputs change over time. Such systems are often referred to as dynamic systems. SIMULINK is very versatile in nature and can be easily and efficiently used to explore the behavior of a

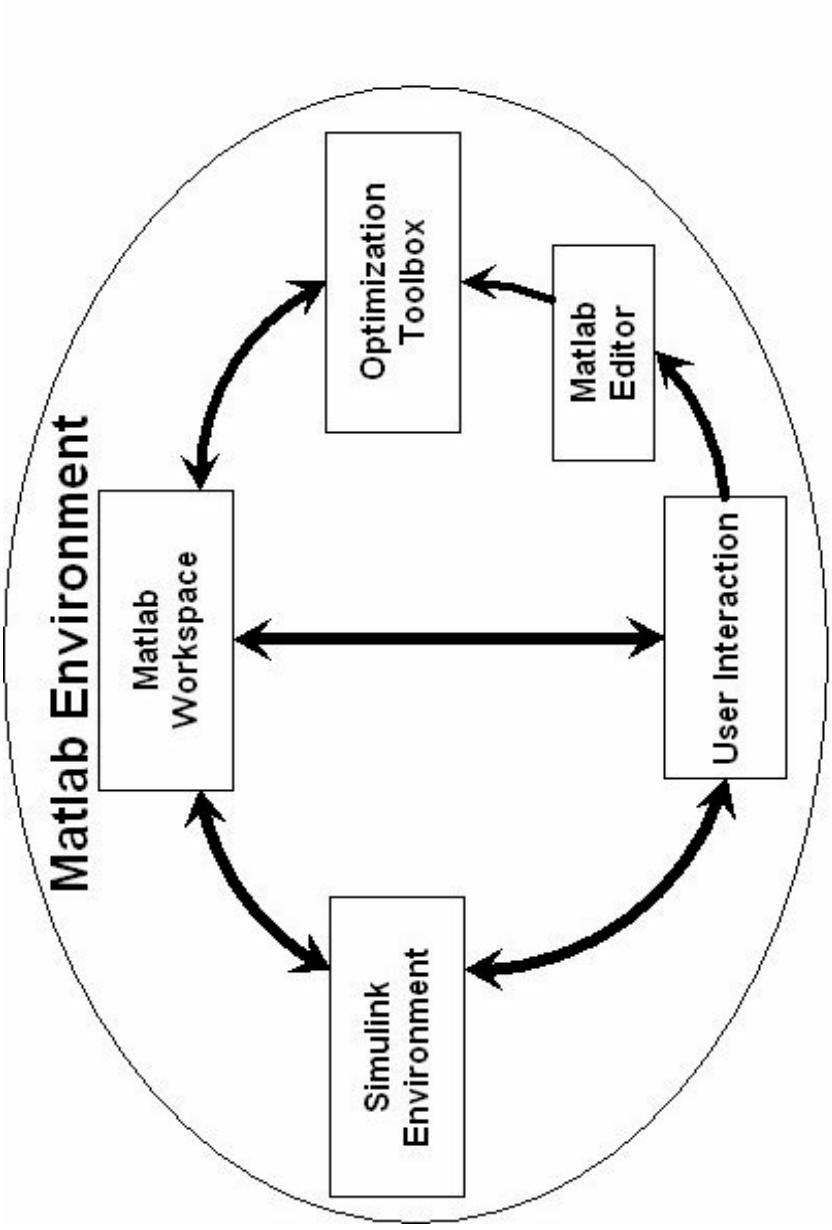


Figure 12. Interaction between various components in MATLAB

wide range of real-world dynamic systems, including electrical circuits, shock absorbers, braking systems, and many other electrical, mechanical, and thermodynamic systems.

Simulating a dynamic system is a two-step process with SIMULINK. First, a graphical model of the system to be simulated is created, using SIMULINK's GUI (Graphical User Interface) model editor. The model depicts the time-dependent mathematical relationships among the system's inputs, states, and outputs. Then, SIMULINK is used to simulate the behavior of the system over a specified time span. SIMULINK uses information that are entered into the model to perform the simulation.

A SIMULINK block diagram is a pictorial model of a dynamic system. Any dynamic equation can be realized as blocks,which are the basic building units in SIMULINK. They are interconnected to each other by lines, which actually carry the signal (data) from one block to another during the course of simulation. Each block produces an output either continuously (a continuous block) or at specific points in time (a discrete block). Every block in a block diagram is an instance of a specific type of block. A block comprises of a set of inputs, states, and outputs. A block's output is a function of time, inputs and the states (if any). The specific function that relates a block's output to its inputs, states, and time depends on the type of block of which the block is an instance. A sample block is illustrated in Figure 13, which shows the estimation of SOC.

There are various library built-in blocks that can assist in mathematical and logical operations, signal generation, data storage and many other functions that one might need during

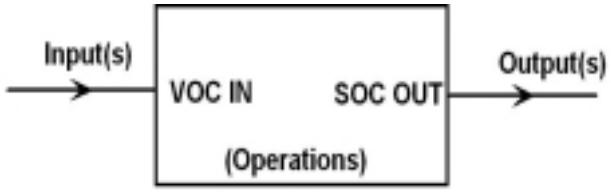


Figure 13. Sample SIMULINK block

a simulation, which makes SIMULINK a very user-friendly environment to work with. The results of the simulation can either be viewed using probes available in SIMULINK or can be exported to the MATLAB workspace for further analysis.

3.4 Function of OPTIMIZATION TOOLBOX

Optimization is the process of finding the minimum or maximum of a function. The OPTIMIZATION TOOLBOX consists of functions that perform minimization (or maximization) on general nonlinear functions. There are various functions using the medium-scale and large scale algorithms to find the minimum (maximum) of a given objective function. The function used in this thesis is $fmincon$ [9], which minimizes the objective function with the given constraints. The simulations run in SIMULINK which is a part of the MATLAB environment. It can be seen that the output of the simulations are the terminal battery voltage and the battery current. In the actual experiment, only these two data can be obtained from ABC-150. The measurements from simulations are then passed on to MATLAB workspace where the data is operated by the OPTIMIZATION TOOLBOX. The toolbox minimizes the error function discussed in the section 2.3 and gives the optimum values for the q parameters. The V_{OC} and SOC can then be derived from the q parameters as mentioned in section 2.4.

3.5 Summary

In this chapter, the methods that were implemented using MATLAB was explained in detail. The basics of MATLAB, SIMULINK, and OPTIMIZATION TOOLBOX were briefly discussed. The next chapter throws light on the real time experiments and ABC-150, an equipment that was used to collect the battery data. Finally the chapter presents the results of the experiments.

Chapter 4
State of Charge estimation with real-time battery data

A set of Hawker Genesis[4] batteries with 16Ah capacity each were used to collect data. The data that was needed for V_{OC} estimation were the discharging current ($I_b(t)$, the battery terminal voltage $V_b(t)$ and the time at which these two parameters were measured. This task was easily accomplished with the help of ABC-150, a programmable battery testing and emulating equipment. Some of the unique features of this equipment are explained in section 4.1. The collected data is then modified so that it could be read by MATLAB. The optimization algorithm is made to run over this data and the output is analyzed. The following sections elaborate this process in detail and present the final results.

4.1 ABC-150-Battery emulator and test equipment

ABC-150 [10] from Aerovironment Inc., is a bidirectional, computer (and/or manually) controlled DC power processing system offering greater accuracy and flexibility. This system has been designed specifically for testing electric and hybrid-electric vehicle batteries. It is controlled through a personal computer (PC) with the help of a special operating system known as ABC-150 ROS (Remote Operating System). ROS is a PC based *graphical user interface (GUI)* application and runs on the Windows NT operating system.

The ABC-150 is an ideal test system for a wide range of DC loads other than bat-

teries and it offers more capability than a traditional power processing system. It is very flexible, which means that the ABC-150 has the ability to follow user defined current, voltage or power profile, within the allowable range. It has two channels, Channel A and B, through which required connections can be made. The ABC-150 interacts with the computer through a series RS-232 link. The ROS checks with the ABC-150 every 15 seconds, and if there is no communication from the ABC-150, then the equipment is set to *standby* mode (no DC power can go in or out of ABC-150 in this mode).

Based on the operating limits, the ABC-150 has three configurations available and they are

- *Independent configuration:* Two channels A and B can be controlled independently in this configuration. For this experiment, the batteries are connected in this configuration because of the flexibility offered by this configuration in controlling the power flow to the batteries through one channel.
- *Parallel configuration:* The two channels A and B use two converters and these two converters are tied together internally to double the maximum current capability. In this configuration, only channel A can be used and no load should be connected to channel B.
- *Differential configuration:* In this configuration, the load is connected between positive terminal of A and B channels while the negative terminals of both the channels are tied together. This configuration allows maximum voltage capability of -420Vdc to

+420Vdc to be applied across the load.

As mentioned earlier, the ABC-150 has the capacity to emulate the batteries. In this mode of operation, the ABC-150 behaves like a battery with the terminal voltage characteristics closely matching the battery characteristics. This is done by first setting the ABC-150 at desired state-of-charge, and then as the current is drawn from the ABC-150, the voltage is lowered as if the battery is discharged. Similarly, as the battery is charged the voltage is increased. The algorithm specifying how voltage should vary can be implemented as a script in ROS, by the user.

4.1.1 ROS Operating system

ROS (*Remote Operating System*) allows the user to control the ABC-150 for manual or automated testing, including test monitoring and data acquisition. It has the ability to run test scripts incorporating drive cycles, the use of an intuitive graphical user interface, and data acquisition integration. With these powerful features, it can be used for testing or cycling EV and HEV batteries and can also be used for other applications. The scripting language is more like C-programming language, and there are various simple commands [10] that can be used very efficiently to perform battery tests. ABC-150 can be controlled either locally at the base or can be controlled remotely with a PC with the help of ROS. The snapshot of ROS graphical test plan is shown in Figure 14.

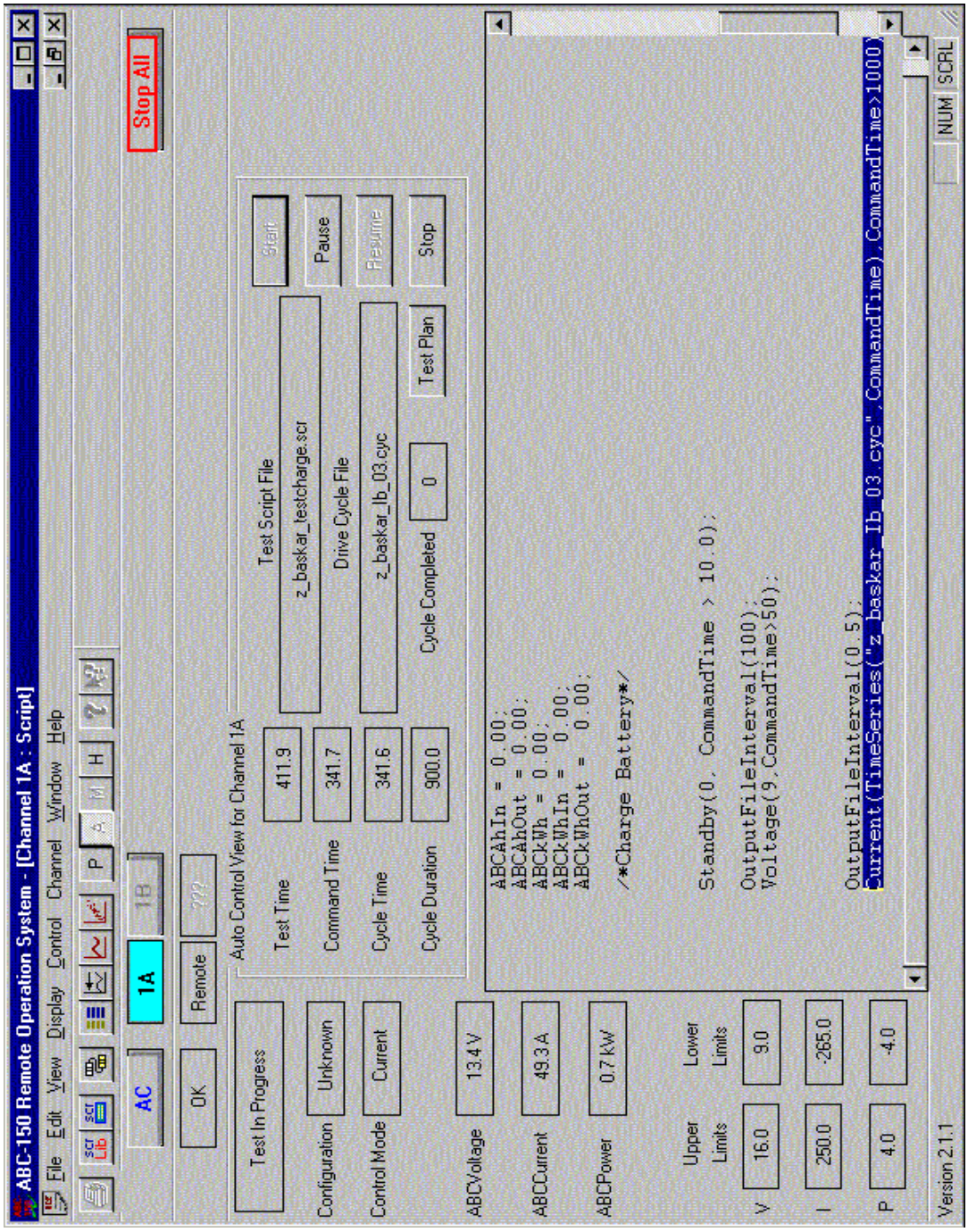


Figure 14. Snapshot of ROS graphical test control

4.1.2 Various modes of operation

A special mode is provided to allow the ABC-150 to be started in Remote or Local or Standby mode. Remote mode allows the user to control the ABC-150 remotely using the computer through ROS. Local mode gives user, the ability to control the ABC-150 unit from the front panel. The Standby mode shuts down the power from the ABC-150 unit, so that no power is given or taken from the load.

There are another set of modes available for charging or discharging the batteries. They are:

- Constant current mode
- Constant voltage mode
- Constant power mode

If one of the ABC-150 parameters, current, voltage or power, is set constant, then the ABC-150 limits the other two parameters so that they do not exceed the limits of operation. Each mode can be used for charging or discharging operation based on the user's need. The discharging current is taken as negative while the charging current is taken as positive by the ABC-150.

4.2 Experimental results

In this section, the actual experimental results will be presented followed by a discus-

sion about the results. The tests were conducted for two different load conditions simulated in ABC-150 and the results are presented here. The battery discharging current and the terminal voltage measurement data were obtained from ABC-150 and formatted to be used by MATLAB. The measured battery discharging current (scaled by a factor of 5), battery terminal voltage and the open circuit voltage of the battery are for the two conditions are illustrated in Figure 15 and 16. It should be noted that while in the actual model the discharging current is taken to be positive, the current is considered to be negative in the actual tests with ABC-150.

The battery terminal voltage, open circuit voltage, and the battery discharging current are plotted on the same graph, to help the reader get a better picture. The actual open circuit voltage is not known during the actual experiments and therefore it was found to be difficult to verify if the V_{OC} estimated was correct. To overcome this difficulty the current waveform is so chosen that it goes to zero and remains there for a some short period of time. This is equivalent to saying that the terminal voltage measured is actually the open circuit voltage since the load current is zero. This helps to cross check the estimated V_{OC}. However, during other time periods when the load current is non-zero the actual V_{OC} is unknown. From Figure 16, one can see that the V_{OC} estimated is very close to the V_b at those intervals when I_b is zero, thus verifying the theory. The comparison of the state of charge and the open circuit voltage of the battery is shown in Figures 17 and 18. In this figures it can clearly be seen that there exists a linear relationship between V_{OC} and SOC of the battery.

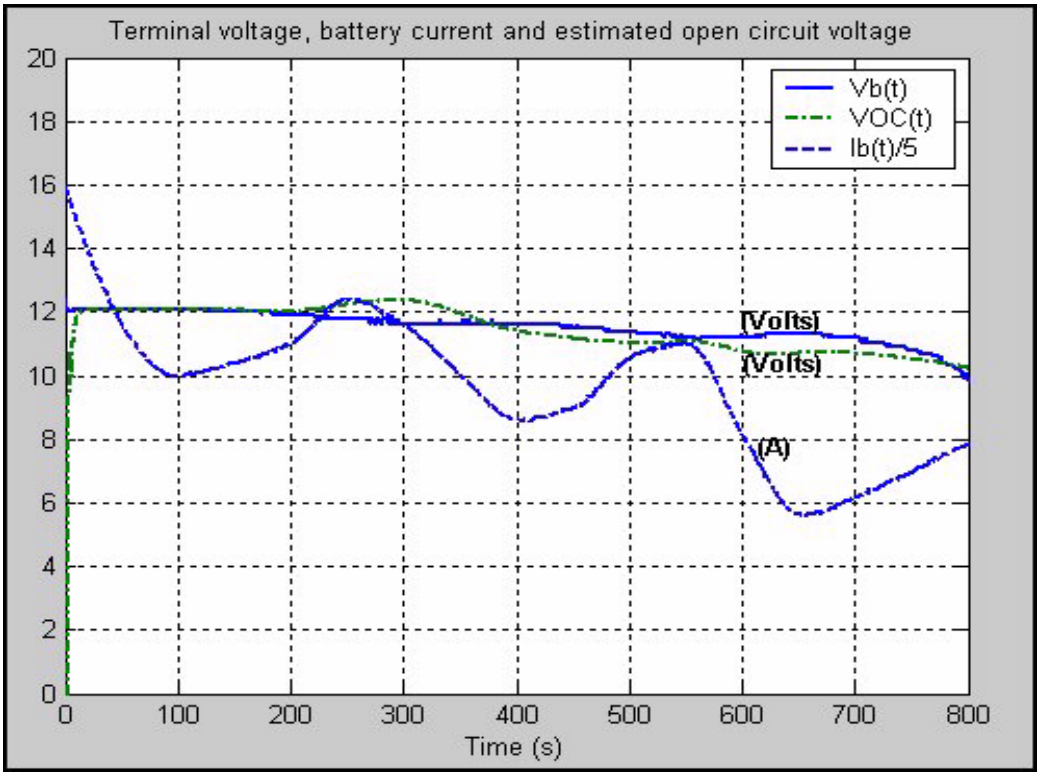


Figure 15. Result - 1: Battery terminal voltage $V_b(t)$, battery current $I_b(t)$ and the estimated open circuit voltage $V_{OC}(t)$ using observability Gramian method

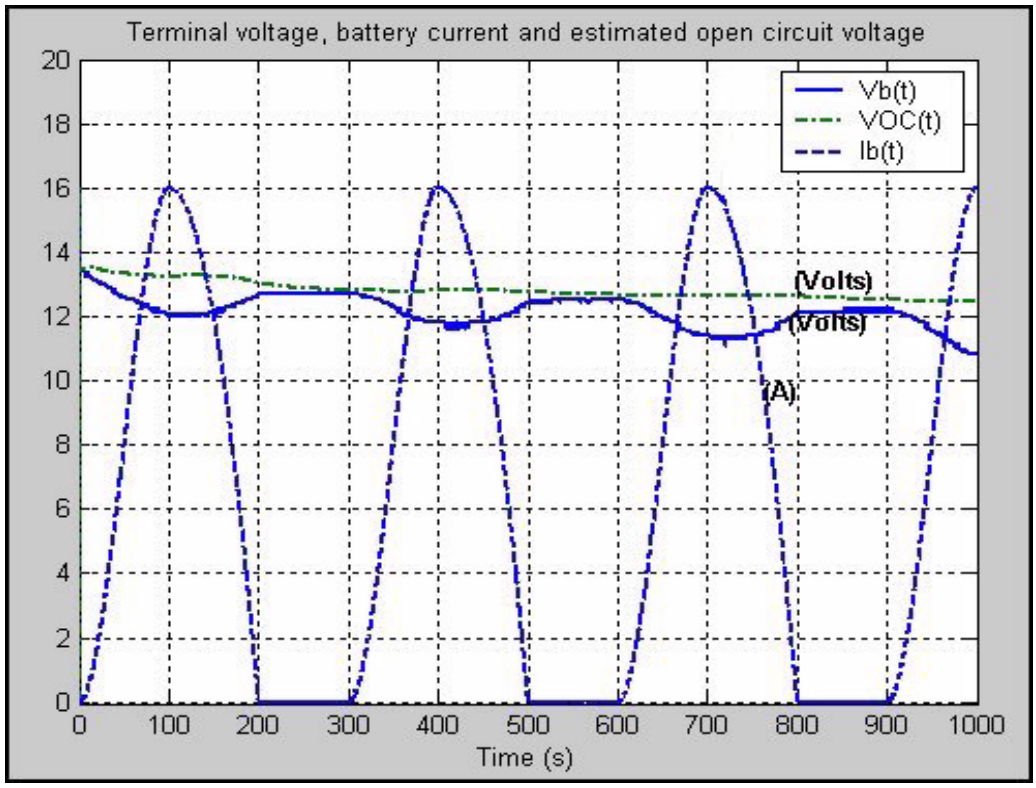


Figure 16. Result - 2: Battery terminal voltage $V_b(t)$, battery current $I_b(t)$ and the estimated open circuit voltage $V_{OC}(t)$ using observability Gramian method

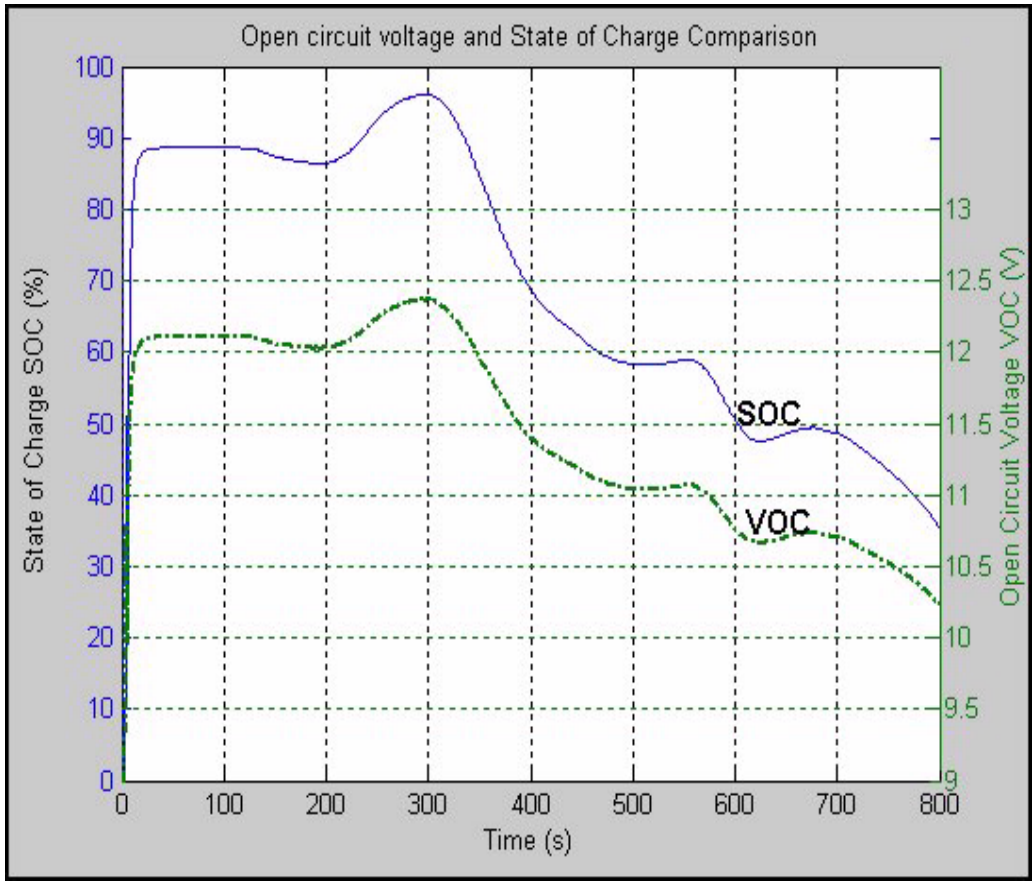


Figure 17. Result - 1: Comparison of V_{OC} and SOC using Observability Gramian method

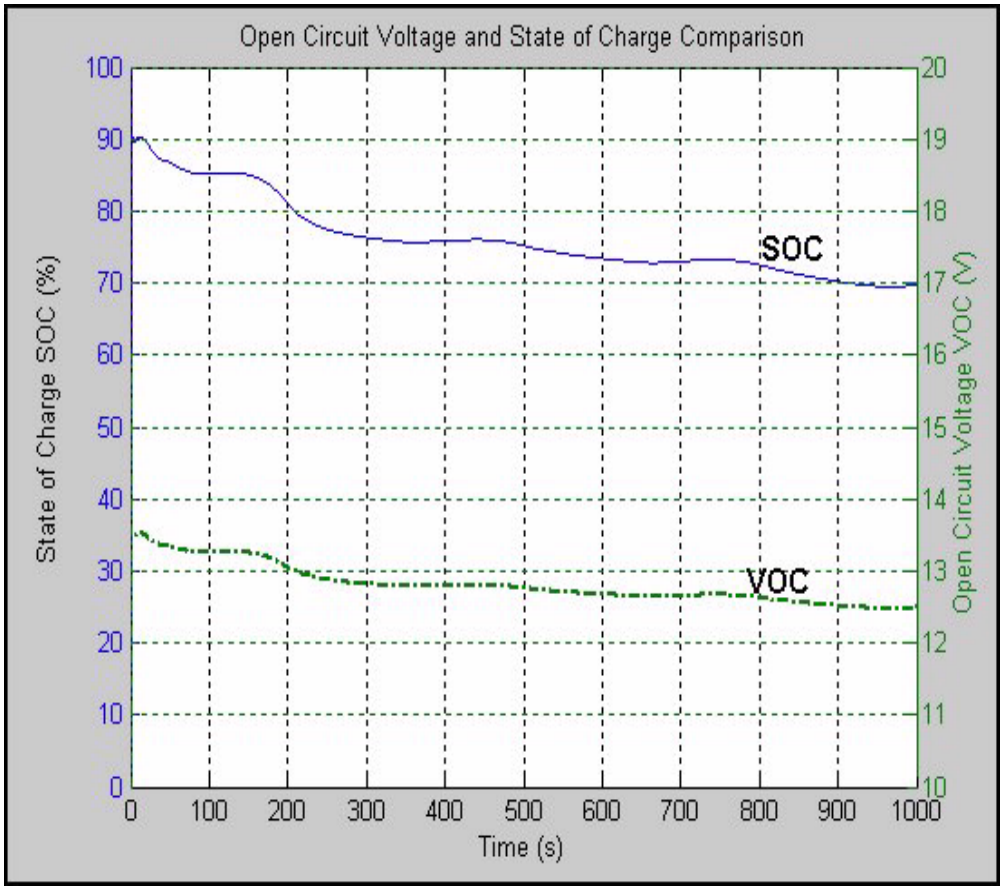


Figure 18. Result - 2: Comparison of V_{OC} and SOC estimated using Observability Gramian method

Chapter 5
Conclusions and Summary

The modified Thevenin equivalent circuit battery model chosen for this thesis gave reasonably good estimation for the state of charge of the battery. In this chapter the procedures adopted in the thesis will be summarized and the conclusion and the scope for possible future work is discussed.

5.1 Summary of the thesis

The objective of this thesis was to estimate the state of charge of the lead-acid batteries with reasonable accuracy. A modified Thevenin equivalent circuit model to represent the lead-acid battery was chosen. In the first method, the equations relating the terminal battery voltage to the other battery parameters such as the internal resistance (R_b), discharging resistance (R_c) and polarization capacitance (C) is derived. The state space model of the battery equivalent circuit is simulated in SIMULINK, and the terminal battery voltage and the discharging current are collected. This data is passed on to OPTIMIZATION TOOLBOX in MATLAB to minimize the error between the estimated terminal voltage and the terminal voltage collected from the simulation. Once the error is minimized, the toolbox gives the optimum values of $q_1, q_2, q_3, q_4\ and\ q_5$ parameters as defined in section 2.3. The open circuit voltage of the battery is then calculated with the help of the q_i's as given in section 2.4. Once the open circuit voltage is found then the state of charge of the battery can

easily be calculated using the linear relationship between them.

In the second method, the non-linear time varying system is reduced to a low order linear time varying system. Then using the observability Gramian the initial states of the state variables and hence V_{OC} are found. It was also shown that the value of V_{OC} is independent of x_{20} over the limit given in Equation (3.75). This method gave results that are very closely matching with the real data that were collected with the ABC-150.

The simulation results gave reasonably accurate results which encouraged to test this numerical algorithm on a real battery. A 16 Ah (Ampere-hours) capacity, sealed lead-acid, Hawker Genesis battery is chosen for experimental purpose. The terminal battery voltage and the discharge current are collected with the help of ABC-150, which is a programmable power processing system. Then, with the help of the observability Gramian method, the open circuit voltage (V_{OC}) and subsequently the state of charge (SOC) of the battery are estimated. The results were found to be comparable to the actual experimental results.

5.2 Conclusion

Few methods were tried to estimate the V_{OC} and SOC of the battery and it was found that the observability Gramian method estimated the V_{OC} and SOC with good accuracy. Even though the results were very satisfactory, there are few points that deteriorates the V_{OC} estimation and they are listed below,

- The polarization capacitance of the battery was not specified by the battery manufacturer, Hawker Energy Products Inc.. This parameter is a crucial parameter in this model because it differentiates the modified Thevenin equivalent circuit model from the rest of the models. An approximate value was chosen for this parameter based on [1].
- The sampling rate of the ABC-150 was another factor which caused problems in the parameter identification. The maximum sampling time that was possible in the ABC-150 was 0.15 seconds. High sampling rate yields very good resolution.
- The terminal voltage measured by the ABC-150 was accurate only up to one decimal place. This resulted in measurement noise, which caused a great problem, because the SOC can vary more than 10% for a small change in open circuit voltage of $0.1V$. This was another reason why this method could not accurately estimate SOC.

If the above mentioned causes for the problems could be alleviated, then this model would estimate the SOC to a greater accuracy.

5.3 Future work

There is a great scope for improvement and future work in this area of battery modeling. If a method could be devised to measure the polarization capacitance of the battery a more accurate estimation is possible. Also, the method discussed throughout the thesis concentrated only on battery discharging so it can equally be applied to battery charging and the results in both the cases could be compared. The battery discharge current is fitted

as a quadratic curve linear in parameters $I_b = a+b(t-t_0)+c(t-t_0)^2$. If the current is fitted into a more complex structure, then this method may yield better SOC approximations.

List of References

[1] Jie Du Shuo Pang, Jay Farrell and Matthew Barth, "Battery state-of-charge estimation," in *Proceedings of the American Control Conference*, Jun. 2001, vol. 2, pp. 1644–1649.

[2] Gelb, *Applied Optimal estimation*, MIT Press, Cambridge,MA., 1974.

[3] R. Rand, D.A.J. Woods and R.M. Dell, *Batteries for Electric Vehicles*, Research Studies Press Ltd., 1998.

[4] Hawker Energy Products Inc., *Genesis Application Manual Fifth edition*, Feb. 2000.

[5] Hawker Energy Products Inc., *Introduction to Batteries*, http://www.hepi.com/basics, 1997.

[6] D. Chan, H.L.and Sutanto, "A new battery model for use with battery energy storage systems and electric vehicles power systems," in *Power Engineering Society Winter Meeting, 2000.IEEE*, Jan. 2000, vol. 1, pp. 470–475.

[7] T. Powell, B.and Pilutti, *Series Hybrid Dynamic Modeling and Control Law Synthesis*, Ford Scientific Research TR SR-93-201, Dec. 1993.

[8] Wilson J. Rugh, *Linear System Theory*, Prentice-Hall,Inc., 1993.

[9] The MathWorks Inc., *MATLAB 6.1*, http://www.mathworks.com, 2002.

[10] *ABC-150 Installation, Operation and Maintenance Manual*, Aerovironment Inc., 1997.

Appendices

Program Files

I - ABC Battery Discharge Script File

```
/* This Program is for the Battery Discharging*/
/* -Baskar Vairamohan- */
/* -Date: 06/07/2002- */
main()
{
	/* INITIALIZATION*/
	int i, j, k;

	float NumberOfModules = 1.0;
	float StartLoop, LoopTime;

	/* SET PROTECTIVE LIMITS FOR ABC-150 */
	Standby(0, CommandTime > 10.0);
	ABCVmin = 9.0 * NumberOfModules;
	ABCVmax = 15.0 * NumberOfModules;
	ABCImin = -265.0;
	ABCImax = 250.0;
	ABCPmin = -4.0 * NumberOfModules;
	ABCPmax = 4.0 * NumberOfModules;
	ChangeLimits(); /* SETS THE ABC-150 LIMITS */
	/* CHANGE THESE VARIABLES ON A COMPUTER CRASH */
	ABCAh	= 0.00;
	ABCAhIn = 0.00;
	ABCAhOut = 0.00;
	ABCkWh	= 0.00;
	ABCkWhIn = 0.00;
	ABCkWhOut = 0.00;

	/*CHARGE BATTERY QUICKLY - DONT COLLECT DATA*/
	Standby(0, CommandTime > 10.0);
	OutputFileInterval(100);
	/* BATTERY IS CHARGED TO 15V IN CONSTANT VOLTAGE MODE*/
	Voltage(15, CommandTime >200);
	OutputFileInterval(0.1); /* SAMPLING TIME = 0.1 SECONDS*/
	/* CURRENT PROFILE FROM z_baskar_Ib_02.cyc IS USED*/
	/* FOR A PERIOD OF 1000 SECONDS */
	Current(TimeSeries("z_baskar_Ib_02.cyc",CommandTime),CommandTime>1000);
	/* COLLECT CURRENT DATA ONLY FOR 1000 SECONDS*/
```

```
    /* GOTO STANDBY AFTER 1000 SECONDS*/
    Standby(0,CommandTime>1000);
}/* END MAIN SCRIPT*/
```

II - MATLAB Files

1. Battery Parameter Identification

```
Program name: bat_param_identify.m
Author: Baskar Vairamohan
Date: 08/14/2002
Function: Identifies the terminal battery voltage parameters by invoking
Optimization toolbox function 'fmincon'
Other functions called:      1. opt_conmin()
                             2. lsq3()
clear all;
clc;
Rb = 7.5e-3; %Ohms
Rd = 7.5e-3; %Ohms
C = 40; %Farads
load kalman_sim_data005; % Loading data file
ca2 = 1/(Rd*C);
ca4 = Rd;
ca5 = Rb;
total_samples = 10000; % samples arbitrarily chosen
n = floor(length(ts)/total_samples); % n gives the total number of
                                     %major segments of the current profile
% Major Segment Looping %
i = 1; NaNCount=0;
VOC_0 = 9;%VOC at SOC = 0%
VOC_100 = 15;% VOC at SOC = 100%
for j = 1:n
    min_t = (j-1)*total_samples+1;
    max_t = j*total_samples;
    t0 = ts(min_t);
    [a,b,c,cond_num] = lsq3(Ib(min_t:max_t),ts(min_t:max_t),t0);% least square
    function called
    %Specify Choice of time interval
    new_samples =100; %new sample intervals
    segments = total_samples/new_samples;
    global new_samples;
    % Minor Segment Looping %
    for z = 1:segments
        min_zt = min_t+(z-1)*new_samples;
        max_zt = min_t+z*new_samples-1;
        if(i == 1)
```

```
        x0 = [9,0 ,0, 0];% initial conditions
else
        x0 = [q1(i-1) q3(i-1) q4(i-1) q5(i-1)];
end
%Global Parameters
global t y t0 t0new;
t0new = ts(min_zt);%t0 is the value of t at the beginning of
                                each minor segment
t = ts(min_zt:max_zt);
y = yk(min_zt:max_zt);
[x_est,fval] = opt_conmin(x0);% this function invokes
                                        optimization toolbox
% Estimated Values
q1e = x_est(1);
q2e = x_est(2);
q3e = x_est(3);
q4e = x_est(4);
q5e = x_est(5);
q1_est(i) = q1e; q2_est(i) = q2e; q3_est(i) = q3e;
q4_est(i) = q4e; q5_est(i) = q5e;
q1(i) = q1e + q3e*(t0new-t0) + q4e*(t0new-t0)^2
q2(i) = q2e;
q3(i) = q3e + 2*q4e*(t0new-t0);
q4(i) = q4e;
q5(i) = q5e*exp(-q2e*(t0new-t0));
% Least square method: Function lsq3() is called
[q1_ls(i), q3_ls(i), q4_ls(i), CondNumY(i)] = lsq3(y,t,t0new);
% New a,b,c Parameters
anew = a + b*(t0new-t0) + c*(t0new-t0)^2;
bnew = b + 2*c*(t0new-t0);
cnew = c;
A_ib(i) = a;
B_ib(i) = b;
C_ib(i) = c;
% New a,b,c's are stored in vectors
Anew(i) = anew;
Bnew(i) = bnew;
Cnew(i) = cnew;
% Ib reconstructed
Ib_est(i) = anew + bnew*[ts(max_zt)-t0new] + cnew*[ts(max_zt)-t0new]^2;
m1_new = -q4(i)/cnew; %c4+c5
c2 = q2(i);
```

```
            n1_new = (q3(i) + bnew*m1_new)/(2*cnew); %c4/c2
            VOC_est(i) = q1(i) + anew*m1_new + n1_new*[bnew + 2*cnew/c2];
            %Least Square V_OC Calculation
            m_ls = -q4_ls(i)/cnew;
            n_ls = (q3_ls(i) + bnew*m_ls)/(2*cnew);
            VOC_ls(i) = q1_ls(i) + anew*m_ls + n_ls*[bnew];
            %SOC Calculation
            SOC(i) = ((VOC_est(i)-VOC_0)*100)/VOC_100;
            %Yk reconstructed
            yk_est(i) = q1(i) + q3(i)*(ts(max_zt)-t0new) + q4(i)*(ts(max_zt)-t0new)^2
                        +q5(i)*exp(-q2(i)*(ts(max_zt)-t0new));
            yk_ls(i) = q1_ls(i) + q3_ls(i)*(ts(max_zt)-t0new)
                        +q4_ls(i)*(ts(max_zt)-t0new)^2;
            i = i+1
        end
end
```

2. Linear Least Square method

Program name: lsq3.m
Author: Baskar Vairamohan
Date: 08/14/2002
Function: This function identifies the linear least square parameters
Other functions called: None
function [a,b,c,cond_num]= lsq3(y,t,t0)
Usage:
[a,b,c]= lsq3(y,t,t0)
y can be anything like current or voltage
y = a + b(t-t0) + c(t-t0)^2
[y] = [W][ABC]
[W] = [W1 W2 W3]
W1 = [1]; W2 = [t-t0's]; W3=[(t-to)^2]

```
len_y=length(y);
len_t=length(t);
if(len_y ~= len_t)
      disp('Length of t and y should be equal');
      break;
end
W1 ones(1,len_y);
W2 = (t-t0);
W3 = [(t-t0).^2];
W = [W1(:) W2(:) W3(:)];
size(W);
tol=1e-3;
Winv = pinv(W,tol);
size(Winv);
size(y);
ABC = Winv*y(:);
a = ABC(1,1);
b = ABC(2,1);
c = ABC(3,1);
cond_num = cond(Winv);
```

III - Optimization Toolbox Files

1. Opt˙conmin.m

Program name: opt_conmin.m
Author: Baskar Vairamohan
Date: 08/14/2002
Function: This function invokes the optimization toolbox to get the optimized parameters
Other functions called: 1. fmincon
function [x_est,fval]= opt_conmin(x0)
Usage:
opt_conmin(a,b,x0)
Function returns: x_est,x_act,fval.
Modified yb(t)=q1+q3(t-t0)+q4(t-t0)^2+q5exp(-q2(t-t0));
Ib(t)=a+b(t-t0)+c(t-t0)^2 profile is assumed
global t y Rd C Rb;
Rd = 7.5e-3; %Ohms
C = 40; %Farads
Rb = 7.5e-3; % Ohms
%Lower and Upper Bounds
LB = [0, 0, 0, 0, 0];
UB = [15, 5, 1, 0.5, 0.8];
fun=@opt_objfun; *%Objective function defined*
[c,fval,exitflag,output]=fmincon(fun,x0,[],[],[],[],LB,UB); % optimization toolbox function
x_est=c;

2. Opt˙objfun.m

Program name: opt_objfun.m
Author: Baskar Vairamohan
Date: 08/14/2002
Function: This function defines the objective function F
Other functions called: None

```
function F=opt_objfun(q)
global y2dot t new_samples t0;
q1 = q(1);
q2 = q(2);
q3 = q(3);
q4 = q(4);
q5 = q(5);
F = 0;
y = y2dot;
new_samples = length(y2dot);
for k = 1:1:new_samples-1
      tk = t(k);
      delta_t = t(k+1)-t(k);
      F = F + [y(k)- (q1 + q2*(tk-t0) + q3*(tk-t0)^2 + exp(-q4*(tk-t0)))]^2*delta_t;
end
F;
```

IV - MATHEMATICA Files

Following is the list of commands that was used to prove $\lim_{(t_f-t_0)\to\infty}(\frac{x_{30}}{x_{20}})$ *is independent of* x_{20}.

$Phi_{11} = Exp[-c2 * (t - t_0)]$
$Phi_{12} = \frac{1}{c_2} * (1 - Exp[-c_2 * (t - t_0)]$
$Phi_{13} = -Integrate[Exp[-c_2 * (t - \tau)] * (a + b * (\tau - t_0) +$
$\quad c * (\tau - t_0)\hat{}2), \{\tau, t_0, t\}]$
$I_b = a + b * (t - t_0) + c * (t - t_0)\hat{}2$
$M_{11} = Integrate[Exp[-2 * c2 * (t - t_0)], \{t, t_0, t_f\}]$
$M_{12} = Integrate[Phi_{11} * Phi_{12}, \{t, t_0, t_f\}]$
$M_{13} = Integrate[Phi_{13}, Phi_{11}, \{t, t_0, t_f\}]$
$M_{14} = -Integrate[Phi_{11} * I_b, \{t, t_0, t_f\}]$
$M_{22} = Integrate[Phi_{12}\hat{}2, \{t, t_0, t_f\}]$
$M_{23} = Integrate[Phi_{12} * Phi_{13}, \{t, t_0, t_f\}]$
$M_{24} = Integrate[-Phi_{12} * I_b, \{t, t_0, t_f\}]$
$M_{34} = Integrate[-Phi_{13} * I_b, \{t, t_0, t_f\}]$
$M_{33} = Integrate[(Phi_{13})\hat{}2, \{t, t_0, t_f\}]$
$M_{44} = Integrate[I_b\hat{}2, \{t, t_0, t_f\}]$
$M_{21} = M_{12}; M_{31} = M_{13}; M_{41} = M_{14}; M_{32} = M_{23}; M_{42} = M_{24}; M_{43} = M_{34}$
$M = \{\{M_{11}, M_{12}, M_{13}, M_{14}\}, \{M_{11}, M_{12}, M_{13}, M_{14}\}, \{M_{11}, M_{12}, M_{13}, M_{14}\},$
$\{M_{11}, M_{12}, M_{13}, M_{14}\}\}$
$M_{new} = M/.t_0 \to 0$; *(Limit* $t_0 \to 0$)
$M_{new2} = M_{new}/.e^{-c_2*t_f} \to 0$
$M_{new2} = M_{new2}/.e^{-2*c_2*t_f} \to 0$
$McInv = Inverse[M_{new2}]$
$Phi = \{\{e^{-c_2 t_k}\}, \{\frac{1-e^{-c_2 t_k}}{c_2}\}, \{\frac{(2c-bc_2+ac_2^2)e^{-c_2 t_k}}{c_2^3} - \frac{2c-bc_2+ac_2^2-2cc_2 t_k+bcc_2^2 t_k+cc_2^2 t_k^2}{c_2^3}\},$
$\quad \{-(a + bt_k + ct_k^2)\}$
$y = q_1 + q_3 * t_k + q_4 * t_k\hat{}2 + q_5 * Exp[-c_2 * t_k]$
$LHS = Integrate[Phi * y, \{t_k, 0, t_f - t_0\}]$
$LHS_{new} = Collect[LHS, e^{c_2(t_f-t_0)}]$
$LHS_{new2} = LHS_{new}/.t_0 \to 0$
$LHS_{new3} = LHS_{new2}/.e^{-c_2*t_f} \to 0$
$LHS_{new4} = LHS_{new3}/.e^{-2*c_2*t_f} \to 0$
$MatrixForm[LHS_{new4}]$
$x_{0new} = McInv.LHS_{new4}$
$x_{02} = x_{0new}[[2, 1]]$
$tmp = Together[x_{02}]$
$tmp_2 = tmp/.q_1 \to c_3 - a * (c_4 + c_5) + b * c_4/c_3 - 2 * c * c_4/(c_2\hat{}2)$

$Together[tmp_2]$
$tmp_3 = tmp_2/.q_3 \longrightarrow -b * (c_4 + c_5) + 2 * c * c_4/c_2$
$Together[tmp_3]$
$Expand[tmp_3]$
$tmp_4 = tmp_3/.q4 \longrightarrow -c * (c_4 + c_5)$
$Expand[tmp_4]$
$Together[tmp_4]$

Vita

Baskar Vairamohan was born in Tiruchirapalli, India. He received his Bachelor of Engineering degree from Anna University, India in 1999. He was an honor student and received a gold medal for academic excellence during his undergraduate studies at the Anna University. After his graduation with a B.E. degree he worked for six months in a software concern as a Programmer analyst. He came to the United States of America in 2000, to pursue his MS degree in Electrical Engineering at The University of Tennessee Knoxville. While he was a student at UT, he served as a Teaching Assistant for the Department of Electrical Engineering tutoring various laboratories which include Digital Signal Processing, Electrical Power Systems, and Electrical Circuit Theory. He was a member of the UT Future Truck team during the year 2000 and served in the modeling and controls division. He currently works at EPRI-PEAC Corporation as a Power Quality Engineer.